Neutralino dark matter, b-τ Yukawa unification, and nonuniversal sfermion masses

S. Profumo*
Scuola Internazionale Superiore di Studi Avanzati (SISSA-ISAS), I-34014 Trieste, Italy
and Istituto Nazionale di Fisica Nucleare, Sezione di Trieste, I-34014 Trieste, Italy
(Received 10 April 2003; published 28 July 2003)

We study the implications of minimal nonuniversal boundary conditions in the sfermion soft supersymmetry breaking (SSB) masses of minimal supergravity. We impose asymptotic b-τ Yukawa coupling unification and we resort to a parametrization of the deviation from universality in the SSB motivated by the multiplet structure of the $SU(5)$ grand unified theory. A set of cosmophenomenological constraints, including the recent results from the Wilkinson Microwave Anisotropy Probe, determines the allowed parameter space of the models under consideration. We highlight a ''new coannihilation corridor'' where $\tilde{\chi}$-$\tilde{b}_1$ and $\tilde{\chi}$-$\tilde{\tau}_1$-$\tilde{\nu}_\tau$ coannihilations significantly contribute to the reduction of the neutralino relic density.

DOI: 10.1103/PhysRevD.68.015006 PACS number(s): 12.60.Jv, 12.10.Kt, 14.80.Ly, 95.35.+d

I. INTRODUCTION

The minimal supersymmetric (SUSY) extension of the standard model (MSSM) and grand unification are often regarded as the main ingredients of physics beyond the standard model [1–3]. The phenomenological implications of the MSSM and of grand unification have been investigated for decades, and, though direct evidence for such theories is still missing, a large set of increasingly stringent constraints has put important bounds on the parameter space of these so-called SUSY grand unified theories (GUTs).

Nonetheless, the theoretical frameworks of SUSY GUTs are countless and typically characterized by a huge number of parameters. The common phenomenological practice is to make a certain number of (hopefully) theoretically motivated assumptions in order to deal with a reduced set of parameters. The first assumption one has to make in the context of SUSY is how to parametrize the mechanism of SUSY breaking.

Here, we resort to one of the most widely studied such contexts, that of the so-called supergravity (SUGRA) models. In this framework, SUSY is broken in a *hidden sector*, whose fields couple only gravitationally to the MSSM fields [4]. Under some further assumptions (gaugino and scalar universality), the soft SUSY breaking part of the Lagrangian of supergravity models is determined by four continuous parameters plus one sign [minimal SUGRA (MSUGRA)].

In this paper, based on the results presented in [5], we study a (*minimal*) deviation from universality in the scalar fermion sector of the theory, inspired by the multiplet structure of the simplest GUT, $SU(5)$ (see Sec. II B). We impose on the model the constraint of b-τ Yukawa coupling unification, which is a common prediction of a wide set of theories of grand unification, among which are the $SU(5)$ and $SO(10)$ GUTs.

One of the virtues of R-parity conserving SUSY models is to produce ideal candidates for cold dark matter [6], in the present case the lightest neutralino (a linear superposition of the neutral gauge and Higgs boson superpartners). The neutralino is, in fact, a color and electromagnetically neutral, weakly interacting massive particle (WIMP), as required to be a good cold dark matter candidate. The recent results from the Wilkinson Microwave Anisotropy Probe (WMAP) satellite [7], combined with other astrophysical data, determined with unprecedented accuracy the dark matter content range of the Universe. It has been shown [8,9] that the cosmologically allowed parameter space of MSUGRA is dramatically restricted by the considerably lowered upper bound on the neutralino relic density. Moreover, as recently pointed out in Ref. [10], in cosmological scenarios involving quintessential fields, the relic density could undergo a further significant enhancement, even of several orders of magnitude. The necessity of efficient relic density suppression mechanisms is therefore by now an uncontroversial point.

One of the known mechanisms of neutralino relic density suppression occurs when the next-to-lightest supersymmetric particle (NLSP) is close in mass to the neutralino. In this case, the neutralino relic density is suppressed not only by neutralino-neutralino annihilations, but also by *coannihilations* with the NLSP, and indirectly also by the annihilations of the NLSP itself [11–13].

This mechanism can involve various sparticles in MSUGRA [14], such as the lightest stau [15–17], top squark [18,19], or chargino [20,16]. In the present paper we address the possibility that minimal nonuniversality in the sfermion sector can produce ''new,'' unusual coannihilation partners. We find that this possibility is effectively realized in what we call a new coannihilation corridor, where the bottom squark and the tau sneutrino play the role of the NLSP. We show that this pattern is compatible with b-τ exact (''top-down'') Yukawa unification (YU), and with all known phenomenological requirements.

In the next section we introduce and motivate the model we analyze. We discuss the issue of b-τ YU and of a GUT-motivated minimal sfermion soft supersymmetry breaking (SSB) mass nonuniversality. We then show in Sec. IV the features of the resulting particle spectrum which give rise to ''new coannihilation corridors'' involving, in addition to the stau, the lightest bottom squark and the tau sneutrino. Section V is devoted to a description of the cosmophenomeno-

*Email address: profumo@sissa.it

logical requirements we apply. We demonstrate in particular that the $\mu>0$ case is not compatible with b-τ top-down YU. In Sec. VI we describe the new coannihilation regions. After our final remarks, we give in the Appendix the complete list of the coannihilation processes involving the neutralino, bottom squark, tau sneutrino, and stau. Finally, an approximate treatment of the neutralino relic density contributions coming from bottom squark–bottom squark, bottom squark–neutralino, and stau–tau sneutrino coannihilations is provided.

II. THE MODEL

A. b-τ Yukawa unification

One of the successful predictions of grand unified theories is the asymptotic unification of the third family Yukawa couplings [1]. The issue of Yukawa unification has been extensively studied; see, e.g., [21–23]. In particular, in this paper we address the issue of YU of the bottom quark and the tau lepton, which is a prediction of some of the minimal grand unification gauge groups, such as $SU(5)$. b-τ YU is a consequence of the fact that the two particles belong to the same $SU(5)$ multiplet, and therefore at the scale of grand unification $M_{\rm GUT}$ they are predicted to have the same Yukawa coupling. The experimental difference between m_τ and m_b is then mainly explained by two effects. First, the renormalization group (RG) running from $M_{\rm GUT}$ to the electroweak scale drives the two masses to different values. Second, in the minimal supersymmetric standard model, the supersymmetric sparticles affect the values of the masses with different finite radiative corrections, in particular, that of the b quark [24].

Previous investigations of b-τ YU include Ref. [25] as regards nonsupersymmetric GUTs and Refs. [26–29], and more recently Refs. [30,31], for the SUSY GUT case. In particular, in [30] the implications of the recent experimental and theoretical results on the muon anomalous magnetic moment and on the inclusive branching ratio $b\to s\gamma$ were also taken into account, while in [32] the neutralino relic density constraint was examined, in the context of gaugino nonuniversality. In Refs. [33–35] the puzzle of the neutrino masses and mixing was tackled within the framework of b-τ YU.

A possible approach to b-τ YU is of the ''bottom-up'' type [29,30]. It consists in defining some parameter which evaluates the *accuracy* of YU, such as

$$\delta_{b\tau}\equiv\frac{h_b(M_{\rm GUT})-h_\tau(M_{\rm GUT})}{h_\tau(M_{\rm GUT})}.$$

The procedure we take here is instead a top-down approach [31,27,28]: for a given set of SUSY parameters we fix the value $h_\tau(M_{\rm GUT})=h_b(M_{\rm GUT})$, requiring the resulting m_τ to be equal to its central experimental value. We then compute $m_b(M_Z)$ through RG running and taking into account the SUSY corrections. A model giving a value of the b-quark mass lying outside the experimental range is ruled out. With this procedure, we perform *exact* b-τ YU at the GUT scale and directly check whether a given model can or cannot be compatible with it.

B. Minimal sfermion nonuniversality

The parameter space of the minimal supersymmetric extension of the standard model, in its most general form, includes more than a 100 parameters [36,37]. Therefore, it is commonly assumed that some underlying principle reduces the number of parameters appearing in the soft supersymmetry breaking Lagrangian. In particular, in the case of gravity-mediated supersymmetry breaking, one can theoretically justify [4] the assumption that there exists, at some high energy scale M_X, a *common* mass m_0 for all scalars as well as a *common* trilinear coupling term A_0 for all SSB trilinear interactions. Moreover, in SUSY GUT scenarios, the additional assumption that the vacuum expectation value of the gauge kinetic function does not break the unifying gauge symmetry yields a common mass $M_{1/2}$ for all gauginos. One is then left with four parameters $(m_0,A_0,M_{1/2},\tan\beta)$ and one sign $(\mathrm{sgn}\,\mu)$, which define the so-called constrained MSSM, or MSUGRA, parameter space.

Much work has been done in the investigation of nonuniversality in the gaugino sector; see, e.g., Refs. [38,39]. As regards the SSB scalar masses, it has long been known that universality is not a consequence of the supergravity framework, but rather an additional assumption [40]. This justified increasing interest in the possible consequences of nonuniversality in the scalar sector [41,42]. In particular, in [43] an analysis of various possible deviations from universality in the SSB was carried out.

In this paper we focus on a simple model exhibiting minimal nonuniversal sfermion mass (MNUSM) at the GUT scale. Our model is inspired by an $SU(5)$ SUSY GUT where the scale of SSB universality M_X is higher than the GUT scale $M_{\rm GUT}$ [43]. The RG evolution of the SSB from M_X down to $M_{\rm GUT}$ induces a pattern of nonuniversality in the sfermion sector dictated by the arrangement of the matter fields in the supermultiplets:

$$(\hat{L},\ \hat{D}^c)\to\overline{\mathbf{5}}, \tag{1}$$

$$(\hat{Q},\ \hat{U}^c,\ \hat{E}^c)\to\mathbf{10}. \tag{2}$$

This structure entails the following pattern of sfermion mass nonuniversality at the GUT scale:

$$m_L^2=m_D^2\equiv m_{\mathbf{5}}^2, \tag{3}$$

$$m_Q^2=m_U^2=m_E^2\equiv m_{\mathbf{10}}^2. \tag{4}$$

The running between M_X and $M_{\rm GUT}$ also produces two other effects. First, a typically large deviation from universality and a splitting between the up and down Higgs boson masses m_{H_1} and m_{H_2} is generated at the GUT scale (a detailed study of nonuniversal Higgs boson masses is presented in [42] and [44]). Second, a small splitting is also present between the SSB masses of the two lightest sfermion families and the third one. In the present paper we will however restrict ourselves to a *phenomenological* parametrization of sfermion nonuniversality, simply setting

$$m_{\mathbf{10}}^2\equiv m_0^2, \tag{5}$$

$$m_{\mathbf{5}}^2 = K^2 m_{\mathbf{10}}^2 = K^2 m_0^2, \tag{6}$$

$$m_{H_1}^2 = m_{H_2}^2 = m_0^2. \tag{7}$$

We are therefore left with a single parameter K, which scans this ''minimal,'' GUT-inspired deviation from universality in the sfermion sector.

For our purposes, we let K vary between 0 and 1: in this way we *recover full universality* [i.e., the constrained MSSM (CMSSM)] for $K=1$, while, for $K<1$, we can lower the spectrum of the sparticles belonging to the $\overline{\mathbf{5}}$ multiplet. Hence, we generate a spectrum with significantly lower masses for the tau sneutrino and the lightest stau and bottom squark. Whenever the masses of these sparticles are close to the neutralino mass, they can play an important role in coannihilation processes.

Being inspired by a SUSY GUT $SU(5)$ framework, it is natural to mention, within the proposed MNUSM model, the critical question of proton decay [45]. First, the nonuniversality pattern of MNUSM is not derived from a definite $SU(5)$ GUT: it simply inherits from this theory a plausible asymptotic soft sfermion mass structure ($m_{\mathbf{10}}^2$ and $m_{\mathbf{5}}^2$) and the feature of b-τ YU. Nonetheless, it has been shown that *consistent* $SU(5)$ models exist [46], where suitable structures for the leptoquark Yukawa couplings h_{QQ}, h_{UE}, h_{UD}, and h_{QL} drastically suppress the proton decay rate, even at large $\tan\beta$. The resulting proton lifetime is then well below the current experimental limits [47]. These consistent models are compatible with the present MNUSM model in the soft SUSY breaking Lagrangian, although for computational ease we take into account here only the third generation Yukawa couplings h_t and $h_b = h_\tau$. Hence, we conclude that MNUSM models, within an $SU(5)$ framework, are viable and are not in contrast with the present constraints on the proton lifetime.

III. NUMERICAL PROCEDURE

The MNUSM model we propose is defined by the following parameters:

$$m_0,\ A_0,\ M_{1/2},\ \tan\beta,\ \mathrm{sgn}\,\mu,\ \text{and}\ K. \tag{8}$$

We impose gauge and b-τ Yukawa coupling unification at a GUT scale M_{GUT} self-consistently determined by gauge coupling unification through two-loop SUSY renormalization group equations [48], both for the gauge and for the Yukawa couplings, between M_{GUT} and a common SUSY threshold $M_{\mathrm{SUSY}} \simeq \sqrt{m_{\tilde{t}_1} m_{\tilde{t}_2}}$ ($\tilde{t}_{1,2}$ are the top squark mass eigenvalues). At M_{SUSY} we require radiative electroweak symmetry breaking, we evaluate the SUSY spectrum, and we calculate the SUSY corrections to the b and τ masses [28]. For the latter we use the approximate formula of Ref. [49]:

$$\frac{\Delta m_\tau}{m_\tau} = \frac{g_1^2}{16\pi^2}\frac{\mu M_2 \tan\beta}{\mu^2 - M_2^2}[F(M_2, m_{\tilde{\nu}_\tau}) - F(\mu, m_{\tilde{\nu}_\tau})], \tag{9}$$

$$F(m_1,m_2) = -\ln\left(\frac{M^2}{M_{\mathrm{SUSY}}^2}\right) + 1 + \frac{m^2}{m^2 - M^2}\ln\left(\frac{M^2}{m^2}\right), \tag{10}$$

$$M = \max(m_1,m_2),\quad m = \min(m_1,m_2). \tag{11}$$

From M_{SUSY} to M_Z the running is continued via the SM one-loop equations (RGEs). We use fixed values [50] for the running top quark mass $m_t(m_t) = 166$ GeV, for the running tau lepton mass $m_\tau(M_Z) = 1.746$ GeV, and for $\alpha_s(M_Z) = 0.1185$, all fixed to their central experimental values. The asymptotic Yukawa couplings $h_\tau(M_{\mathrm{GUT}}) = h_b(M_{\mathrm{GUT}})$ and $h_t(M_{\mathrm{GUT}})$ are then consistently determined to get the correct top and tau masses, while the tree level m_b^{tree} and the SUSY-corrected m_b^{corr} masses of the running bottom quark at M_Z are outputs.

The neutralino relic density is computed by interfacing the output of the RGE running with the publicly available code MICROMEGAS [51], which includes thermally averaged exact tree level cross sections of all possible (co)annihilation processes, an appropriate treatment of poles, and the one-loop QCD corrections to the Higgs boson coupling with the fermions. The output of MICROMEGAS also produces the relative contributions of any given final state to the reduction of the neutralino relic density.

The direct and indirect detection rates are estimated through another publicly available numerical code, DARKSUSY [52].

As regards the phenomenological constraints, the Higgs boson masses are calculated using MICROMEGAS [51], which incorporates the FEYNHIGGSFAST code [53], where the SUSY contributions are calculated at two loops. The inclusive $\mathrm{BR}(b \to s\gamma)$ is again calculated with the current updated version of the MICROMEGAS code [54], where the SM contributions are evaluated using the formalism of Ref. [55] and the charged Higgs boson SUSY contributions are computed including the next-to-leading order SUSY QCD resummed corrections and the $(\tan\beta)$-enhanced contributions (see Ref. [56]). The SUSY contributions to the muon anomalous magnetic moment δa_μ are directly calculated from the formulas of Ref. [57] and compared with the output of the MICROMEGAS code.

IV. THE PARTICLE SPECTRUM WITH MNUSM

In minimal supergravity, especially after the very precise results from the WMAP satellite [7], giving a considerably reduced upper limit on the cold dark matter density of the Universe, the cosmologically allowed regions of the parameter space are strongly constrained [8,9]. As pointed out in [58,59], two main mechanisms can suppress the neutralino relic density to sufficiently low values. The first one is coannihilation of the neutralino with the next-to-lightest sparticles, which is effective whenever the mass of the latter lies within 10–20 % of the neutralino mass [60,11,12]. The second mechanism is given by direct, rapid s-channel annihilation of the neutralino with the CP-odd Higgs boson A [61], which takes place if $m_A \simeq 2m_{\tilde{\chi}}$, i.e., if the channel is en-

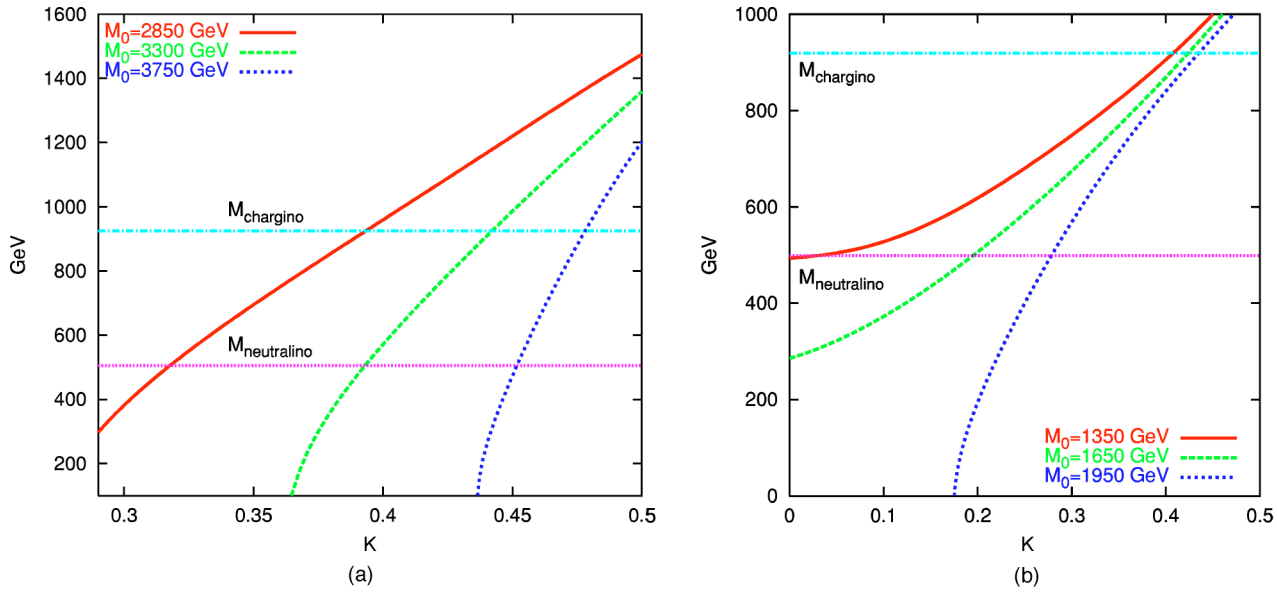

FIG. 1. The bottom squark (a) and sneutrino (b) spectrum at $M_{1/2}=1.1$ TeV, $\tan\beta=38.0$, and $A_0=0$ for different values of m_0.

hanced by pole effects.[1] In particular, we choose to focus here on the case of coannihilations, which in the present scenario of MNUSM are expected to exhibit a rich pattern.

In order to understand the possible pattern of coannihilations emerging from the parametrization of sfermion mass nonuniversality outlined in Sec. II B, we study the spectrum of the candidate NLSPs, namely, the lightest bottom squark and the tau sneutrino. The dependence of the masses of these two sparticles on the high energy SSB inputs can be parametrized as follows:

$$m^2_{\tilde{b}_1} \simeq a_{\tilde{b}_1} K^2 m_0^2 + (b_{\tilde{b}_1} m_0^2 + c_{\tilde{b}_1} M^2_{1/2} + \Delta_{\tilde{b}_1}), \qquad (12)$$

$$m^2_{\tilde{\nu}_\tau} \simeq a_{\tilde{\nu}_\tau} K^2 m_0^2 + (b_{\tilde{\nu}_\tau} m_0^2 + c_{\tilde{\nu}_\tau} M^2_{1/2} + \Delta_{\tilde{\nu}_\tau}). \qquad (13)$$

The contributions $\Delta_{\tilde{b}_1,\tilde{\nu}_\tau}$ originate in part from $SU(2)_L$ and $U(1)_Y D$-term quartic interactions of the form $(\text{squark})^2(\text{Higgs boson})^2$ and $(\text{slepton})^2(\text{Higgs boson})^2$, and are proportional to $\cos(2\beta)M_Z^2$ [2]. The bottom squark mass gets a further contribution in $\Delta_{\tilde{b}_1}$ arising from the LR off-diagonal elements of the mass matrix. The mixing terms are generated by the typically large values of A_b, in its turn induced, even for $A_0(M_{\rm GUT})=0$, by RG running, and by a $(\tan\beta)$-enhanced contribution proportional to μm_b. In the case of the tau sneutrino, instead, a further, though small, contribution to $\Delta_{\tilde{\nu}_\tau}$ analogously arises from A_τ.

We plot in Figs. 1(a) and 1(b) the typical behaviors of the sparticle masses as functions of K, at fixed $M_{1/2}$, m_0, and $\tan\beta$. Frame (a) shows the case of the mass of the bottom squark (we also plot the corresponding masses of the lightest neutralino and chargino). The high energy parameters are fixed at $M_{1/2}=1100$ GeV, $\tan\beta=38.0$, $A_0=0$, and $m_0=2850$, 3300, and 3750 GeV. We clearly see from the figure that the behavior is, as expected, $m_{\tilde{b}_1} \approx \sqrt{\alpha+\beta K^2}$, where $\alpha<0$ is the sum of the terms in parentheses in Eq. (12) and $\beta=a_{\tilde{b}_1} m_0^2>0$. Increasing the value of m_0 induces higher negative values for α, as well as obviously higher values for β. Notice in any case that for sufficiently low values of K the mass of the bottom squark is driven *below* the mass of the neutralino and also to negative values.

Frame (b) shows instead the mass of the tau sneutrino, at $M_{1/2}=1100$ GeV, $\tan\beta=38.0$, $A_0=0$, and $m_0=1350$, 1650, and 1950 GeV. We see that here also $m_{\tilde{\nu}_\tau} \approx \sqrt{\alpha+\beta K^2}$, but in this case the interplay between $b_{\tilde{\nu}_\tau}$ and $c_{\tilde{\nu}_\tau}$ generates α either positive ($m_0=1350$,1650 GeV) or negative ($m_0=1950$ GeV). The outcome is therefore that the sneutrino mass can be lowered toward the mass of the neutralino for low values of K, depending on m_0; the typical range of m_0 for which this is possible is always lower than in the bottom squark case.

We carried out a thorough investigation of the possible coannihilation regions, and we found that a good parameter is represented by the ratio $(m_0/M_{1/2})$ at fixed $\tan\beta$, $M_{1/2}$, and A_0. In Fig. 2 we plot the coannihilation corridors that we found on scanning the plane $(m_0/M_{1/2},K)$ at $M_{1/2}=1.1$ TeV, $\tan\beta=38.0$, and $A_0=0$. Within the solid lines $(m_{\rm NLSP}-m_{\tilde{\chi}})/m_{\tilde{\chi}} \lesssim 20\%$. In the lower part of the figure, which we indicate as an "Excluded Region," the low value of m_0 implies that the stau becomes lighter than the neutralino, or even gets a negative (unphysical) mass. Very stringent bounds [62] indicate that the LSP has to be electrically and color neutral, and therefore this region is excluded. The

[1]Since here $m_A \simeq m_H$, where H is the heaviest CP-even neutral Higgs boson, the condition $m_A \approx 2m_{\tilde{\chi}}$ implies pole effects for H also. However, since the CP quantum number of the exchanged Higgs boson must match that of the initial state, only A exchange contributes to the S wave, while H (and h) contribute to the P wave. This implies a suppression, in the thermally averaged cross section, of a factor $3/x_F \approx 0.1$–0.2 (see the Appendix).

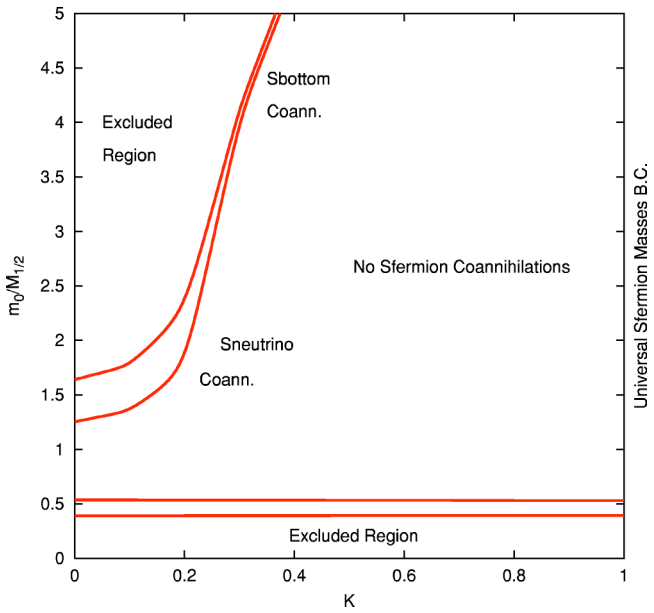

FIG. 2. Coannihilation regions in the $(m_0/M_{1/2},K)$ plane at $M_{1/2}=1.1$ TeV, $\tan\beta=38.0$, and $A_0=0$. Points within the lines are characterized by $(m_{\rm NLSP}-m_{\tilde\chi})/m_{\tilde\chi}\lesssim 20\%$. In the top left and lower parts of the figure the LSP is not a neutralino, while in the top right region no coannihilations take place between the neutralino and the sleptons.

strip above this excluded region represents a first coannihilation corridor, where the NLSP is the stau. We notice that this region survives up to $K=1$, i.e., fully universal boundary conditions. It actually represents a slice of the narrow band, in the $(m_0,M_{1/2})$ plane, which is cosmologically allowed because of neutralino-stau coannihilations (see, e.g., Figs. 1 and 2 of Ref. [8]).

For values of $K\lesssim 0.5$ we find a second, distinct, branch where the mass of the NLSP lies within 20% of the LSP mass. In the lower part of the branch (in Fig. 2 up to $m_0/M_{1/2}\approx 3$), the NLSP turns out to be the tau sneutrino, with the lightest stau which is quasidegenerate with it (say within a few percent; see the discussion in Sec. VI B). Increasing m_0 and moving to the upper part of the branch, the lightest bottom squark becomes the NLSP, while the tau sneutrino and the stau, still quasidegenerate, become much heavier. In the upper left part of the figure, once again indicated as an "Excluded Region," either the bottom squark or the tau sneutrino becomes lighter than the neutralino, or even gets a negative value for its mass (see Fig. 1).

In Fig. 3 we study the dependence of the shape of the coannihilation corridors on the various parameters that we fixed in Fig. 2. In frame (a) we vary the values of $M_{1/2}$, comparing the $M_{1/2}=1100$ GeV case of Fig. 2 with, respectively, $M_{1/2}=1600$ GeV and $M_{1/2}=600$ GeV. We see that there is almost no significant dependence of the shape on the value of $M_{1/2}$, and therefore we conclude that the chosen parameter $m_0/M_{1/2}$ is good, since it is $M_{1/2}$ quasi-independent. In frame (b) we vary instead the value of the universal trilinear coupling A_0. We plot again with a solid line the $A_0=0$ case, as well as the $A_0=1$ TeV and $A_0=-1$ TeV cases, always at $\tan\beta=38.0$ and $M_{1/2}=1100$ GeV. Once again we do not see any significant effect, apart from a common shift of the lower coannihilation branch upward and of the upper downward. These shifts can be traced back to the effect of the off-diagonal A_0 (sign-independent) entries in the sfermion mass matrices.

Figure 4 illustrates the dependence on $\tan\beta$, highlighting this time a significant effect on the upper branch: increasing $\tan\beta$ yields higher values for K, i.e., the branch is moved to the right, and vice versa. This effect can be qualitatively understood from the approximate expression for the mass eigenvalues of the relevant sfermions, Eq. (12), where an increase in $\tan\beta$ is compensated by an increase in the effective boundary value of the scalar masses, tuned by the pa-

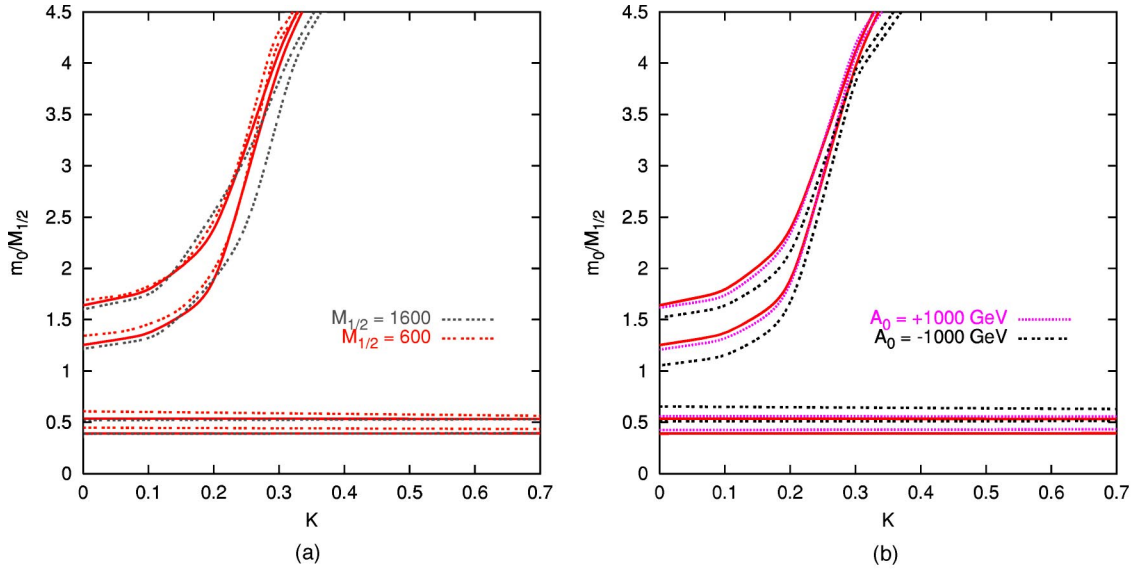

FIG. 3. Coannihilation regions in the $(m_0/M_{1/2},K)$ plane at $\tan\beta=38.0$ and $A_0=0$. In frame (a) the dependence on $M_{1/2}$ is studied at $A_0=0$. In frame (b) two different values for the trilinear coupling $A_0=\pm 1$ TeV are plotted at $M_{1/2}=1100$ GeV.

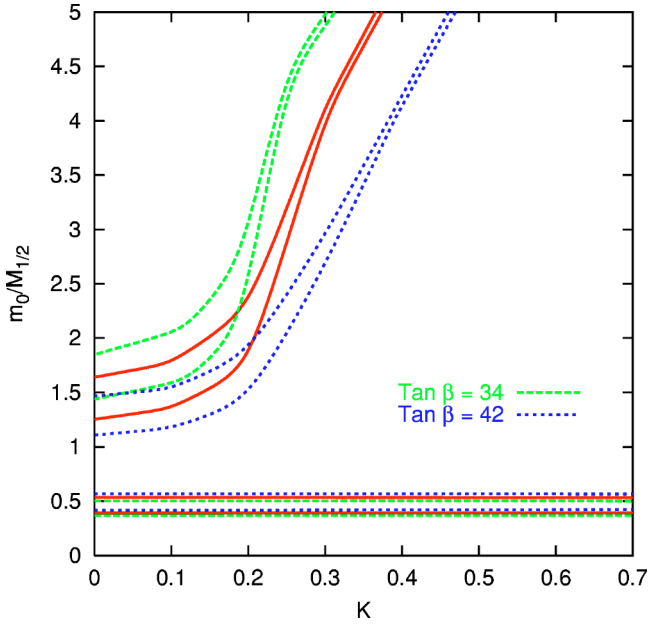

FIG. 4. Coannihilation regions in the $(m_0/M_{1/2},K)$ plane at $M_{1/2}=1.1$ TeV and $A_0=0$. The solid lines indicate the coannihilation corridor for $\tan\beta=38.0$, while the dashed and dotted lines indicate, respectively, $\tan\beta=34$ and 42.

rameter K. For instance, $\Delta_{\tilde{b}_1}$ contains a negatively contributing term proportional to $\tan\beta m_b\mu$, which is compensated, when the values of m_0 and $m_{\tilde{\chi}}$ are fixed, by an increase of K.

V. COSMOPHENOMENOLOGICAL BOUNDS

In this paper we apply two classes of constraints: on the one hand, we apply the cosmological bounds coming from the limits on the cold dark matter content of the Universe and from direct and indirect neutralino searches; on the other hand, we impose the most stringent "accelerator" constraints, such as the inclusive BR($b\to s\gamma$) and the Higgs boson mass. In this second class we also include the bound on the b-quark mass, direct sparticle searches, and a conservative approach [63] to the constraint coming from the SUSY corrections to the muon anomalous magnetic moment δa_μ.

For illustrative purposes, we show the behavior of three *benchmark* cases, pertaining to the three regions of coannihilation highlighted in the previous section. That is, we choose three representative values of K and require the mass splitting between the neutralino and the NLSP to be 10%. We then scan the parameter space, setting $A_0=0$ and $\mu<0$ for simplicity and varying $m_{\tilde{\chi}}$. The features of the three cases considered are summarized in Table I.

TABLE I. The three benchmark scenarios described in the text.

NLSP	$\Delta_{\rm NLSP}$	K	$\tan\beta$
Stau	0.1	0.8	36.0
Bottom squark	0.1	0.4	36.0
Tau sneutrino	0.1	0.2	36.0

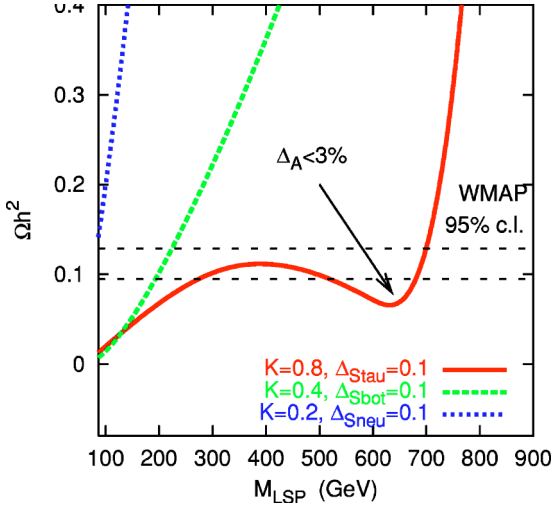

FIG. 5. Neutralino relic density for the three benchmark cases of Table I. The upper and lower bounds on $\Omega_{\rm CDM}h^2$ are the 95% C.L.s from a WMAP global fit [7].

A. Neutralino relic density confronting WMAP results

Supersymmetric models with conserved R parity generate ideal candidates for cold dark matter, such as, in the present case, the lightest neutralino. It is therefore natural to require, in addition to the satisfaction of the other phenomenological constraints, that the cosmological relic density of the neutralinos lies within the bounds indicated by cosmology. In particular, the recent results from the WMAP satellite [7], combined via a global fit procedure with other astrophysical data (including other cosmic microwave background experiments, LSS surveys, and the Ly α data), give a compelling bound on the cosmological relic density of cold dark matter:

$$\Omega_{\rm CDM}h^2=0.1126^{+0.00805}_{-0.00905}. \tag{14}$$

We take here the 2σ range, and we require that $\Omega_{\tilde{\chi}}h^2\lesssim 0.1287$. Strictly speaking, the lower bound cannot be directly imposed, if we suppose that the neutralinos are not the only contributors to the cold dark matter of the Universe. For illustrative purposes, in Fig. 11 below we plot also the lower bound on the relic density.

In Fig. 5 we show instead the behavior of the neutralino relic density as a function of $m_{\tilde{\chi}}$ for the three benchmark cases. We see that in the case of the tau sneutrino the coannihilations contribute only weakly to the reduction of the relic density (see Sec. VI B), which, as expected, diverges quadratically with $m_{\tilde{\chi}}$. In the case of the bottom squark coannihilation, SUSY QCD effectively enhances the relic density suppression, which nonetheless still exhibits a divergent behavior. In the case of the stau, instead, we notice how the interplay between coannihilation and direct rapid annihilation through the A-pole s channel can drastically reduce the relic density. In the dip located between 600 and 700 GeV, in fact, the splitting between the mass of the CP-odd Higgs boson and twice the mass of the neutralino $(m_A-2m_{\tilde{\chi}})/2m_{\tilde{\chi}}\lesssim 3\%$, and therefore direct pole annihilations are extremely efficient, leading to viable values of $\Omega_{\tilde{\chi}}h^2$ for rather high $m_{\tilde{\chi}}\lesssim 700$ GeV.

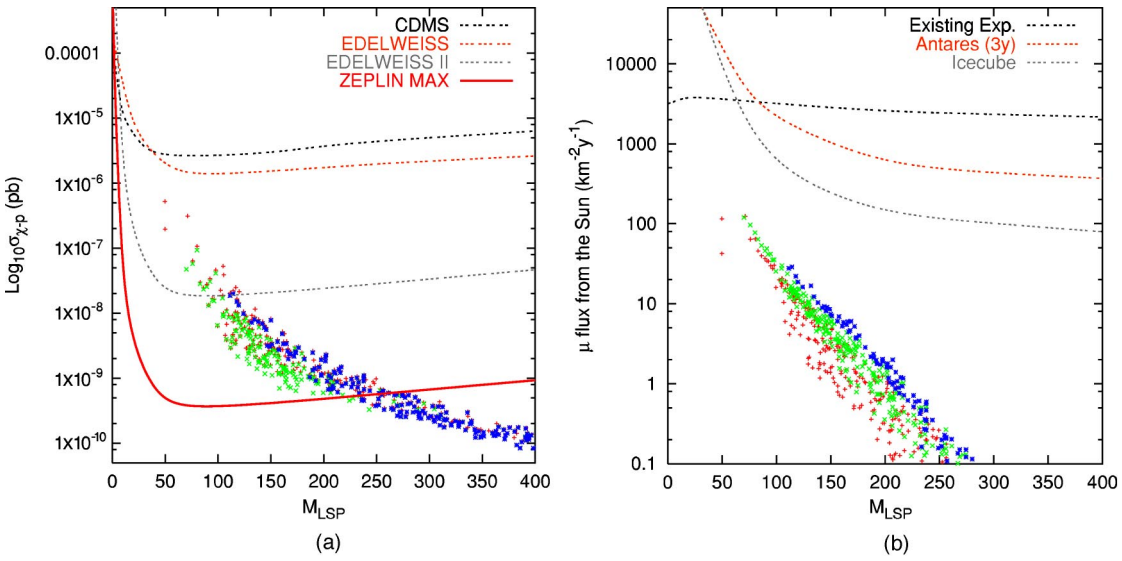

FIG. 6. Direct (a) and indirect (b) detection rates for $K=1.0$ (+, full universality), $K=0.35$ ($\times$), and $K=0.1$ (*). The points refer to $50<M_{1/2}<1000$ GeV, $20<m_0<3000$ GeV, and $-500<A_0<500$ GeV, at $\tan\beta=38.0$. In frame (a) we plot $\sigma^{\rm scal}_{\tilde\chi\text{-}q}$ and the sensitivity bounds of present and future direct detection experiments [64]. In frame (b) we report the neutralino annihilation induced muon flux from the Sun, in $\mathrm{km}^{-2}\,\mathrm{y}^{-1}$, and we compare again with current and future indirect detection experiment sensitivities [65].

B. Direct and indirect WIMP searches

As pointed out in [39], nonuniversality in the sfermion sector should not give rise to substantial modifications to $\sigma^{\rm scal,spin}_{\tilde\chi\text{-}q}$. In fact, owing to the small Yukawa couplings of the lightest generation of quarks, NUSMs do not greatly affect the masses of the up and down squarks, leading to effectively unchanged values for the direct annihilation cross sections, sensitive to processes like $\tilde\chi_q \xrightarrow{\tilde q} \tilde\chi_q$. Further, we find that Higgs boson exchange processes do not give rise, in the MNUSM models, to sizable contributions, as compared with the fully universal case. In Fig. 6(a) we scatter-plot the spin-independent cross section $\sigma^{\rm scal}_{\tilde\chi\text{-}q}$ as a function of $m_{\tilde\chi}$ for $K=1.0$ (+, full universality case), $K=0.35$ ($\times$), and $K=0.1$ ($*$). We randomly scan the parameter space for a given value of K with $50<M_{1/2}<1000$ GeV, $20<m_0<3000$ GeV, and $-500<A_0<500$ GeV, fixing $\tan\beta=38.0$, and requiring the satisfaction of the phenomenological constraints. We also include the sensitivities of present and future direct detection experiments [64]. Notice that some MNUSM models lie within the reach of future direct detection experiments. As far as indirect detection (e.g., the muon flux from the Sun) is concerned, nonuniversality does not significantly affect the detection rates, although t-channel sfermion exchange is enhanced by lighter third generation sfermions for $K<1$, as we can see in Fig. 6(b): for smaller values of K we obtain larger muon fluxes from the Sun. Present and future indirect detection experiments [65] are however sensitive to muon fluxes well above what we obtain for MNUSM models.

To summarize, we find, for both direct and indirect detection, that the MNUSM scenario produces detection rates in the same range as the CMSSM [66], and therefore (minimal) sfermion nonuniversality can hardly be inferred from WIMP searches. Further, present experimental bounds do not constrain the models under consideration.

C. SUSY corrections to the b-quark mass

It has already been pointed out (see, e.g., [30,31]), that the requirement of b-τ Yukawa unification favors negative[2] values of μ. We recall that $\mathrm{sgn}\,\mu$ is one of the parameters included both in the CMSSM and in our MNUSM model. In this section we demonstrate that, even with MNUSM, $\mu>0$ is not compatible with YU. We then discuss the $\mu<0$ case which allows, in a suitable $\tan\beta$ range, the satisfaction of b-τ YU.

The main problem of b-τ YU with $\mu>0$ is that one typically obtains a tree level mass for the b quark which is close to the experimental upper bound, and one has to add on top of it large *positive* SUSY corrections [Eq. (16)], which drive $m_b^{\rm corr}$ outside the experimental range (or, the other way round, h_b far away from h_τ, in the bottom-up approach). We impose b-τ YU at the GUT scale, we fix $h_\tau(M_{\rm GUT})=h_b(M_{\rm GUT})$ from the properly corrected and RG-evolved $m_\tau(M_Z)$, obtaining as outputs the tree level $m_b^{\rm tree}$ and the SUSY-corrected $m_b^{\rm corr}$ masses of the running bottom quark at M_Z. We compare these numbers with the appropriately evolved b-quark pole mass [68] up to the M_Z scale, with $\alpha_s(M_Z)\simeq 0.1185$, following the procedure of Refs. [69,70]:

$$m_b(m_b)=4.25\pm0.3\ \mathrm{GeV}\Rightarrow m_b(M_Z)=2.88\pm0.2\ \mathrm{GeV}. \tag{15}$$

The largest SUSY corrections arise from bottom squark–gluino and top squark–chargino loops, frozen at the $M_{\rm SUSY}$ scale [24,49,71]. They are *nondecoupling effects* because one

[2]We use here the standard sign conventions of Ref. [67].

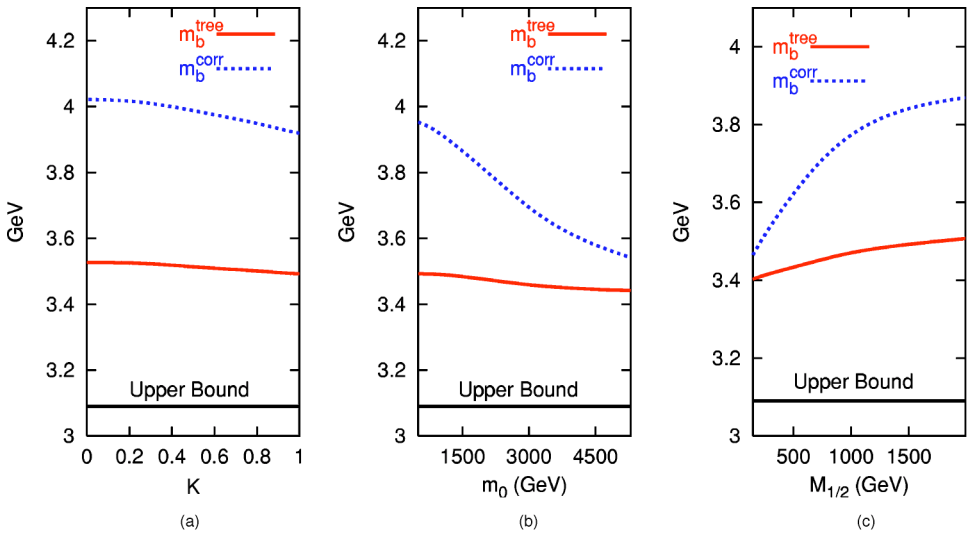

FIG. 7. Tree level and SUSY-corrected values of the b-quark mass at $\tan\beta=38.0$ and $A_0=0$. In frame (a) the parameter K is varied at fixed $M_{1/2}=1100$ GeV and $m_0=1000$ GeV. In frame (b) m_0 is varied at fixed $M_{1/2}=1100$ GeV and $K=1$. Frame (c) shows the dependence on $M_{1/2}$ at $m_0=2000$ GeV and $K=1$.

gets a finite contribution even in the infinite sparticle mass limit, and they can be cast in the following approximate form:

$$\frac{\Delta m_b^{\tilde{g}}}{m_b} \approx \frac{2\alpha_s}{3\pi} M_3 \mu I(m_{\tilde{b}_1}^2, m_{\tilde{b}_2}^2, M_3^2) \tan\beta, \tag{16}$$

$$\frac{\Delta m_b^{\tilde{\chi}^-}}{m_b} \approx \frac{h_t^2}{16\pi^2} \mu A_t I(m_{\tilde{t}_1}^2, m_{\tilde{t}_2}^2, \mu^2) \tan\beta, \tag{17}$$

$$I(x,y,z) \equiv \frac{xy\ln(x/y) + xz\ln(z/x) + yz\ln(y/z)}{(x-y)(y-z)(x-z)}. \tag{18}$$

Unless the trilinear coupling A_t is very large, the gluino loop typically dominates (an exception is investigated in Ref. [72]) and the sign of the SUSY contribution is given by the sign of $M_3\mu$. Therefore, since we assume here gaugino universality, this implies that b-τ YU is favored in the $\mu<0$ case.

To numerically quantify this statement, we study the behavior of $m_b^{\rm tree}$ and $m_b^{\rm corr}$ on varying the parameters of the MNUSM model. In Fig. 7(a) we fix $A_0=0$, $\tan\beta=38.0$, $m_0=1000$ GeV, and $M_{1/2}=1100$ GeV and analyze the dependence on K. Wee see that the tree level value $m_b^{\rm tree}$ is roughly constant, while the SUSY corrections *decrease* as K increases. Both remain well above the experimental upper bound, however. This can be understood from Eq. (16), since increasing K means increasing $m_{\tilde{b}_1}$, with a fixed value for M_3 and, roughly, for μ and $m_{\tilde{b}_2}$, and the function $I(x,y,z)$ at fixed y and z is inversely proportional to $x=m_{\tilde{b}_1}$. Therefore, subsequently, we concentrate on the *universal* $K=1$ case, in order to check whether or not a parameter space allowing for top-down b-τ YU exists.

The second step is to study the dependence of the b-quark mass on the parameter m_0 [Fig. 7(b)]. We take here $A_0=0$, $\tan\beta=38.0$, $M_{1/2}=1100$ GeV, and $K=1$, and we notice, as expected, that the size of the corrections decreases with increasing m_0. This is explained on the one hand by the fact that from the radiative electroweak symmetry breaking (EWSB) condition the value of μ^2 is slightly decreased by the increase of m_0 [2], and on the other hand because increasing the value of $m_{\tilde{b}_{1,2}}$ leads to a decrease of the function I. In Fig. 7(c) we take instead $A_0=0$, $\tan\beta=38.0$, $m_0=2000$ GeV, and $K=1$ and vary $M_{1/2}$. As can be easily inferred from Eq. (16), increasing $M_{1/2}$ leads to an increase both in M_3 and in μ. In conclusion, the candidate parameter space for b-τ YU for $\mu>0$ is at low $M_{1/2}$ and high m_0 values. We choose therefore two trial values, $M_{1/2}=300$ GeV, $m_0=2000$ GeV, and show our results in Fig. 8. As is readily seen from Eq. (16), we find that the SUSY contributions grow with $\tan\beta$. We notice, however, that the tree level mass strongly decreases with increasing $\tan\beta$, owing to the fact that the positive SUSY contributions to m_τ [see Eq. (9)] imply a smaller value for the asymptotic common b-τ Yukawa coupling. The overall combination of these two effects maintains the corrected b-quark mass well above the experimental upper bound. This conclusion is further confirmed by investigating extreme values of $(M_{1/2}, m_0)$ for high $\tan\beta$, always in the universal $K=1$ case, and resorting also to nonzero values of A_0.

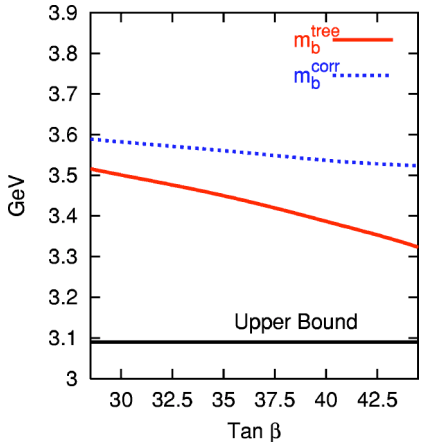

FIG. 8. Tree level and SUSY-corrected values of the b-quark mass at $M_{1/2}=300$ GeV, $m_0=2000$ GeV, $A_0=0$, and $K=1$.

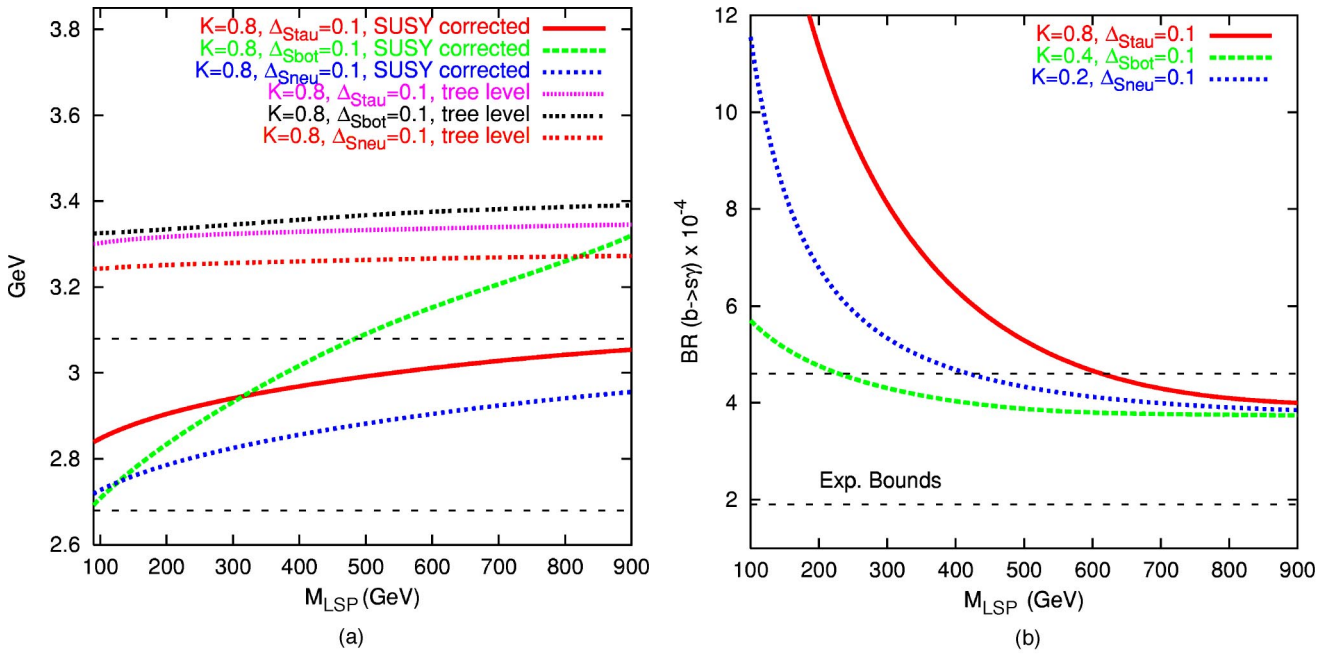

FIG. 9. Tree level and SUSY-corrected b-quark masses (a) and BR($b\to s\gamma$) for the three benchmark scenarios of Table I. The upper and lower bounds are those of Eq. (15) for frame (a) and those of Eq. (19) for frame (b).

To sum up, we demonstrated that, due to the SUSY corrections to the b-quark mass, top-down b-τ YU is excluded, both with universal and with minimal nonuniversal sfermion masses, in the case $\mu>0$.

The $\mu<0$ case

In the $\mu<0$ case the SUSY contributions to the b-quark mass are negative and therefore combine to bring the tree level mass dictated by b-τ YU *within* the experimental range (15). We plot in Fig. 9(a) the tree level and SUSY-corrected values of the b-quark mass for the three benchmark cases of Table I. We notice that the size of the SUSY corrections decreases when $m_{\tilde{\chi}}$ is increased, because of the mentioned behavior of the function $I(x,y,z)$ of Eq. (16), which is inversely proportional to its arguments. In the case of the bottom squark coannihilation (dashed line) the effect is enhanced by the large size of m_0, which directly reduces, through the suppression of μ due to the EWSB condition, the size of the SUSY contributions.

D. The inclusive branching ratio $b\to s\gamma$

We construct the 95% C.L. range on BR($b\to s\gamma$) starting from the recent experimental data of Ref. [73] and properly combining the experimental and theoretical uncertainties. The resulting bound is

$$1.9\times 10^{-4}\lesssim \mathrm{BR}(b\to s\gamma)\lesssim 4.6\times 10^{-4}. \tag{19}$$

We calculate BR($b\to s\gamma$) using the current updated version of MICROMEGAS [54]. The SM contribution is calculated through the formulas of Ref. [55], and the SUSY corrections through those of Ref. [56]. We can estimate the dependence of the SUSY corrections from the approximate formulas of Refs. [74,48,75]. They are given, respectively, for the charged Higgs boson and for the chargino exchanges, by

$$C^{H^+}\approx \frac{1}{2}\frac{m_t^2}{m_{H^+}^2} f^{H^+}\left(\frac{m_t^2}{m_{H^+}^2}\right), \tag{20}$$

$$C^{\tilde{\chi}^-}\approx (\mathrm{sgn}\, A_t)\frac{\tan\beta}{4}\frac{m_t}{\mu}\left[f^{\tilde{\chi}^-}\left(\frac{m_{\tilde{t}_1}^2}{\mu^2}\right) - f^{\tilde{\chi}^-}\left(\frac{m_{\tilde{t}_2}^2}{\mu^2}\right)\right], \tag{21}$$

where

$$f^{H^+}(x)=\frac{3-5x}{6(x-1)^2}+\frac{3x-2}{3(x-1)^3}\ln x, \tag{22}$$

$$f^{\tilde{\chi}^-}(x)=\frac{7x-5}{6(x-1)^2}-\frac{x(3x-2)}{3(x-1)^3}\ln x. \tag{23}$$

We notice that the relative sign of the two contributions of Eqs. (20) and (21) is given by $\mathrm{sgn}(A_t\mu)=-\mathrm{sgn}(M_3\mu)$ (this equality being valid for large top and bottom Yukawa couplings, as in the present case). Moreover, the SM contribution has the same sign as the charged Higgs boson one. All the contributions *decrease* as $m_{\tilde{\chi}}$ increases; therefore we expect to draw a lower bound on $m_{\tilde{\chi}}$ from the lower bound on BR($b\to s\gamma$) [Eq. (19)] in the case $M_3\mu>0$ and from the upper bound of Eq. (19) for $M_3\mu<0$, which is the present case. We notice that the lower bound on $m_{\tilde{\chi}}$ becomes more restrictive as $\tan\beta$ is increased, as can be read from Eq. (21).

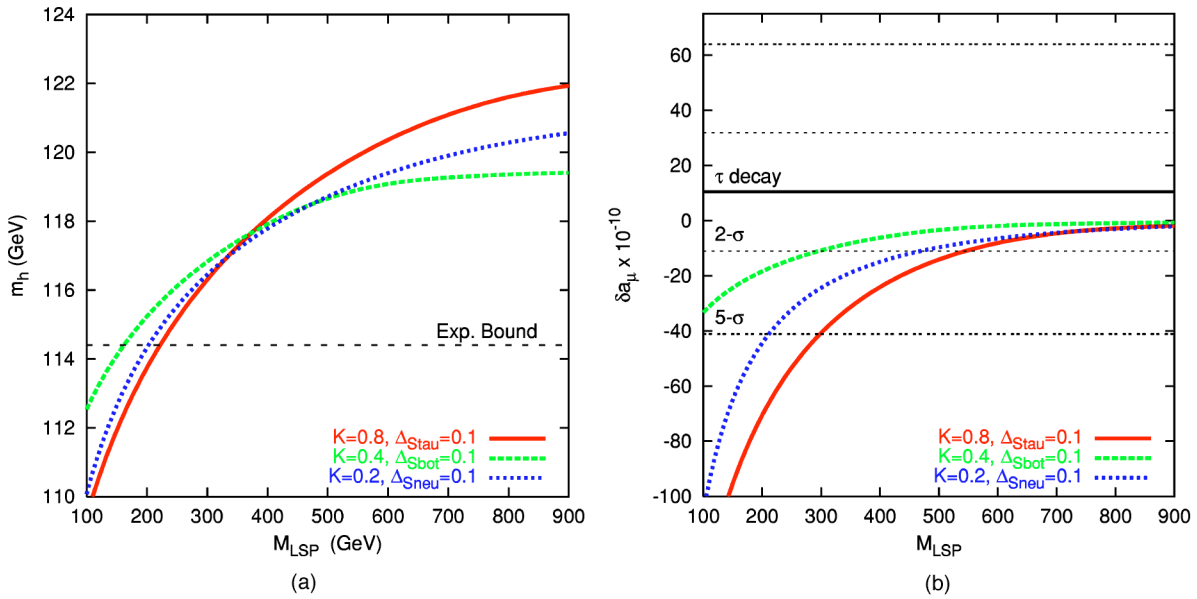

FIG. 10. m_h (a) and δa_μ^{SUSY} (b) for the three benchmark scenarios of Table I. The lower bound of frame (a) is given in Eq. (24), while in frame (b) the 2σ and 5σ bounds are taken from Eq. (27).

In Fig. 9(b) we plot the results we get for the three benchmark cases of Table I. We can see that as the SUSY spectrum becomes heavier (we recall that if the bottom squark is the NLSP $m_0/M_{1/2} \gtrsim 3$; see Fig. 2) the lower bound on $m_{\tilde{\chi}}$ weakens, as can be understood from Eqs. (20) and (21) and from the explicit forms of f^{H^+} and $f^{\tilde{\chi}^-}$.

E. The Higgs boson masses

We take in our analysis the 95% C.L. CERN e^+e^- collider LEP bound [76] on the lightest *CP*-even neutral Higgs boson mass,

$$m_h \gtrsim 114.3 \text{ GeV}, \tag{24}$$

which gives a lower bound on the $m_{\tilde{\chi}}$. Two-loop corrections are taken into account, as described in Sec. III. In Fig. 10(a) we plot the results for the Higgs boson mass that we obtain for the three benchmark scenarios.

F. Direct accelerator sparticle searches

We impose the current direct accelerator search limits on the sparticle masses [50], $m_{\chi_1^+} \gtrsim 104$ GeV, $m_{\tilde{f}} \gtrsim 100$ GeV for $\tilde{f} = \tilde{t}_1, \tilde{b}_1, \tilde{l}^\pm, \tilde{\nu}$, and $m_{\tilde{g}} \gtrsim 300$ GeV, $m_{\tilde{q}_{1,2}} \gtrsim 260$ GeV for $\tilde{q} = \tilde{u}, \tilde{d}, \tilde{s}, \tilde{c}$. We always find the constraints from BR($b \to s\gamma$) and from m_h more restrictive than those from the direct sparticle searches. Therefore we do not plot these bounds in the figures of Secs. VI A and VI B.

G. The muon anomalous magnetic moment

The deviation δa_μ of the muon anomalous magnetic moment a_μ from its predicted value in the standard model can be interpreted as arising from SUSY contributions, $\delta a_\mu^{\text{SUSY}}$, mainly given by neutralino-smuon and chargino-sneutrino loops. The quantity $\delta a_\mu^{\text{SUSY}}$, which we compute numerically with the MICROMEGAS package, can be estimated through the formulas of Ref. [57], assuming a common value for the SUSY sparticles masses m_{SUSY}:

$$\delta a_\mu^{\text{SUSY}} \approx \text{sgn}(M_2 \mu) \frac{\tan\beta}{192\pi^2} \frac{m_\mu^2}{m_{\text{SUSY}}^2} (5g_2^2 + g_1^2). \tag{25}$$

On the experimental side, the BNL E821 experiment recently delivered a high precision measurement (0.7 ppm) of $a_\mu^{\text{expt}} = 11659203(8) \times 10^{-10}$. The theoretical computation of the SM prediction is plagued by the problem of estimating the hadronic vacuum polarization contribution. In particular, there is a persisting discrepancy between the calculations based on the τ-decay data and those based on low energy e^+e^- data. Recent evaluations [77–79] give the following range for the deviation of the SM value of a_μ from the experimental one:

$$a_\mu^{\text{expt}} - a_\mu^{\text{SM}} = (35.6 \pm 11.7) \times 10^{-10} \quad (e^+e^-), \tag{26}$$

$$a_\mu^{\text{expt}} - a_\mu^{\text{SM}} = (10.4 \pm 10.7) \times 10^{-10} \quad (\tau \text{ decay}). \tag{27}$$

Following the lines of Ref. [63], we decided to take a conservative approach to the problem of choosing which bound should be culled from the tantalizing results of Eqs. (26), (27). In what follows we will therefore just indicate the region determined by the 2σ and 5σ ranges for the e^+e^--based approach and for the τ-decay-based approach, but we will not use this constraint to derive (lower) bounds on $m_{\tilde{\chi}}$.

In Fig. 10(b), where we present the results we get for the three benchmark scenarios, we indicate only the τ-decay-based limit, since $\delta a_\mu^{\text{SUSY}}$, with $\mu < 0$, is negative

[see Eq. (25)]. In passing, we remark that it has been recently claimed [79] that the result from e^+e^- data (26) is less clean than the one from τ decay (27). This would be due to interferences of isoscalar $I=0$ mesons, not produced in τ decay, with vector mesons [79]. Therefore, theories requiring a negative sign of μ, such as those with exact b-τ YU, seem to be no longer disfavored by the δa_μ constraint.

Formula (25) allows us to interpret the results we show in Fig. 10(b) and in the figures of the next section. First, we see that as the SUSY spectrum becomes heavier (bottom squark NLSP case) the corrections become smaller, as emerges from Eq. (25). Second, we can see that $\delta a_\mu^{\rm SUSY}$ decreases with increasing $m_{\tilde\chi}$, for the same region as above, and that it increases with increasing $\tan\beta$.

VI. THE NEW COANNIHILATION CORRIDOR

In the $\mu<0$ case the SUSY corrections to the b-quark mass are negative, and therefore can naturally drive, for suitable values of $\tan\beta$, the corrected $m_b^{\rm corr}(M_Z)$ within the experimental range.

In this section we focus on the extended sfermion coannihilation modes allowed by the particle spectrum of the MNUSM model. As pointed out in Sec. IV, the boundary conditions given by MNUSM produce a new "coannihilation branch," extending from $K=0$ up to $K\approx 0.5$ and, for values of m_0 greater than $\approx cM_{1/2}$, with c of $o(1)$, increasing with decreasing values of $\tan\beta$. In the upper part of the branch, typically for $m_0/M_{1/2}\gtrsim 3$, the NLSP turns out to be the lightest bottom squark, while for $c\lesssim m_0/M_{1/2}\lesssim 3$ we find $m_{\tilde\chi}\simeq m_{\tilde\nu_\tau}\simeq m_{\tilde\tau_1}$. The following two subsections are devoted to analysis of the coannihilation processes $\tilde\chi$-$\tilde b_1$ and $\tilde\chi$-$\tilde\nu_\tau$-$\tilde\tau_1$, taking into account the constraints described in the previous section. The final two subsections deal, respectively, with the determination of the $\tan\beta$ range allowed by b-τ YU and with the question of fine-tuning in MNUSM models.

A. $\tilde\chi$-$\tilde b_1$ coannihilation

Since it is a strongly interacting particle, we find that bottom squark annihilation and coannihilation channels are very efficient and contribute substantially to the neutralino relic density suppression.

We plot in Figs. 11 and 12(a) and 12(b) the cosmologically allowed regions for three representative values of $\tan\beta=34$, 38, and 42 for a fixed value of $K=0.35$. The y axis represents the relative percent splitting between the neutralino mass and the next-to-lightest SUSY particle, in this case the lightest bottom squark:

$$\Delta_{\rm NLSP}=\frac{m_{\rm NLSP}-m_{\tilde\chi}}{m_{\tilde\chi}}. \tag{28}$$

The relevant phenomenological constraints described in the previous sections determine lower, and sometimes upper, limits on $m_{\tilde\chi}$. They result in almost vertical lines, since they typically weakly depend on m_0, which moreover varies very little in the plotted regions. They are instead fixed by $M_{1/2}$

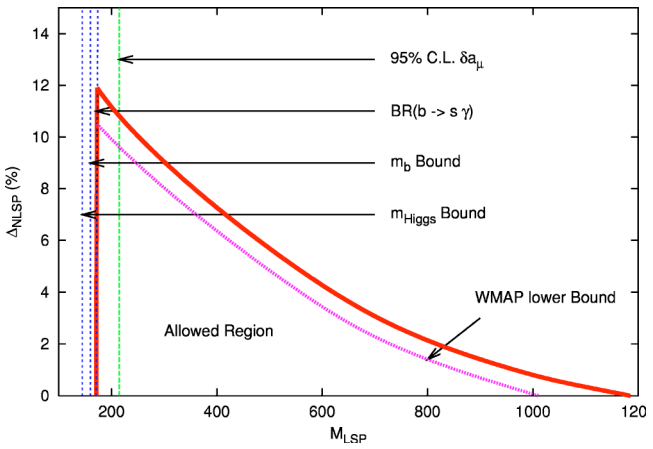

FIG. 11. Cosmologically allowed parameter space in the bottom squark coannihilation region, at $K=0.35$ and $\tan\beta=38.0$. The region below the solid line has $\Omega_{\tilde\chi}h^2<0.1287$. The dotted line shows the putative lower bound on the neutralino relic density (14). The dotted nearly vertical lines indicate the phenomenological constraints described in the text, while the dashed line stands for the 2σ bound on the muon anomalous magnetic moment.

(and therefore, in the plots, by $m_{\tilde\chi}$). The regions allowed by a given constraint lie at the *right* of the corresponding lines. Points below the solid lines are characterized by relic densities which fall within the 2σ range of Eq. (14). We emphasize that the limits on $m_{\tilde\chi}$ and $\Delta_{\rm NLSP}$ that we find here cannot be regarded as being representative of the full parameter space: they show instead, for a few benchmark cases, how the interplay of the cosmophenomenological bounds described in Sec. V constrains the mass spectrum (here parametrized by $m_{\tilde\chi}$ and $\Delta_{\rm NLSP}$) of the models under consideration.

In Fig. 11 we plot with a dotted line the lower bound on $\Omega_{\rm CDM}h^2$ also. We see that the most stringent bound, for $\tan\beta\lesssim 38$, is provided by BR($b\to s\gamma$), while for higher values of $\tan\beta$ the b-quark mass constraint becomes more restrictive. As far as the upper bound on $m_{\tilde\chi}$ is concerned, we find that high values of $\tan\beta$ allow $m_{\tilde\chi}$ to extend up to 1.5 TeV [Fig. 12(b)]. For smaller $\tan\beta$ the upper bound on $m_{\tilde\chi}$ is instead fixed by the upper bound on the b-quark mass: the SUSY corrections to m_τ [see Eq. (9)] drive the common b-τ Yukawa coupling to higher values, therefore generating a higher tree level b-quark mass which is not compensated by the (smaller) negative SUSY corrections to m_b [Eq. (16)]. The inverse mechanism pushes the lower bound on $m_{\tilde\chi}$ to higher values (≈ 0.5 TeV) in the case of $\tan\beta=42$. We notice that the region determined by the 2σ δa_μ range from the τ-decay approach always covers the greater part (or the totality) of the allowed parameter space.

In Fig. 13 we studied the sensitivity of our results to a nonzero value of the common trilinear coupling A_0 at the GUT scale, for $\tan\beta=38.0$, $\Delta_{\tilde b_1}\simeq 0$, and $K=0.35$. We notice that the lower limit on $m_{\tilde\chi}$ is fixed by the $A_0=0$ case. As for the cosmological bound on $\Omega_{\tilde\chi}h^2$, the variation of A_0 leads to very little modification of the upper bounds on $m_{\tilde\chi}$ displayed in Figs. 11 and 12; we therefore conclude that the only relevant change is the type of constraint that, depending on the sign and on the absolute value of A_0, determines the lower bound on $m_{\tilde\chi}$.

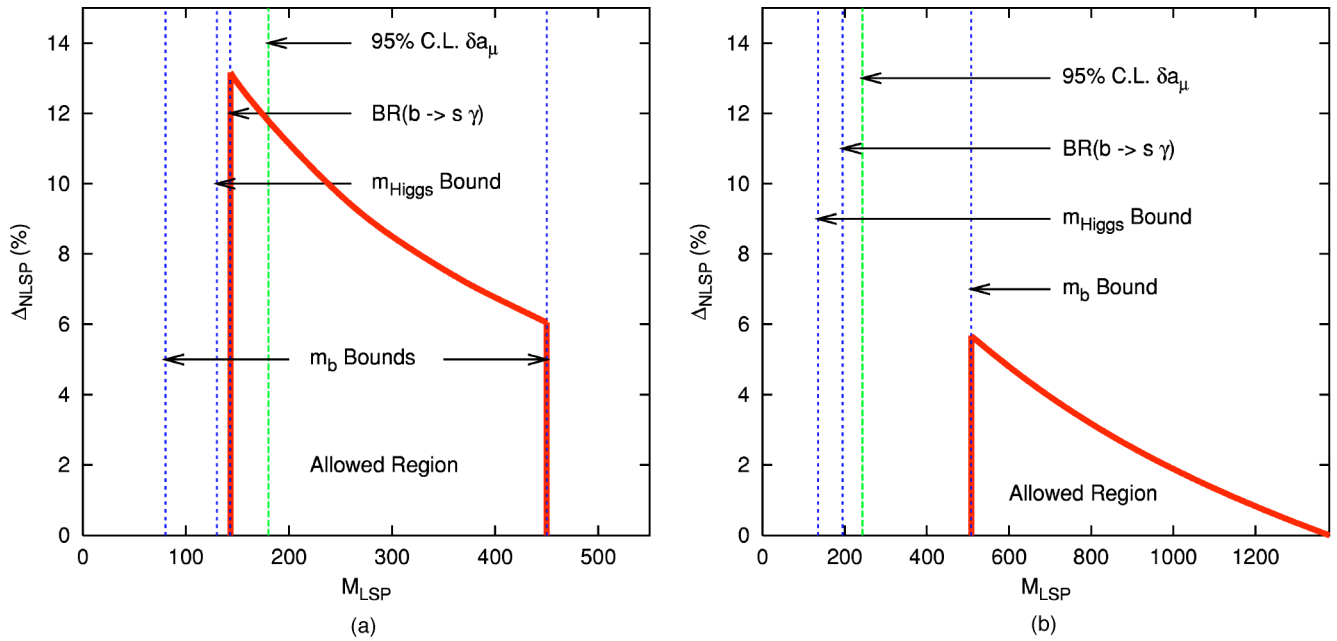

FIG. 12. Cosmophenomenologically allowed parameter space in the bottom squark coannihilation region at $K=0.35$, $\tan\beta=34.0$ (a) and $\tan\beta=42.0$ (b).

As far as the coannihilation channels are concerned, the case of the bottom squark is characterized by a rather simple pattern, clearly dominated by strong interaction processes. We find that for bottom squark masses quasidegenerate with the neutralino mass, the neutralino pair annihilation rate is very low (less than a few percent). The dominant channels concern instead neutralino–bottom squark coannihilations into gluons and b quarks (up to 10%) and bottom squark–bottom squark annihilations into two b quarks (up to 15%) or into two gluons (up to 80%). We give in the Appendix (Sec. A 2) an approximate analytical treatment of these three most relevant processes.

B. $\tilde{\chi}$-$\tilde{\tau}_1$-$\tilde{\nu}_\tau$ coannihilations

In the lower part of the new coannihilation branch of Fig. 2, for $(m_0/M_{1/2})\lesssim 3$ and $0<K\lesssim 0.25$, the NLSP switches from the bottom squark to the tau sneutrino. In this region the lightest stau is always heavier than the sneutrino, but the relative mass splitting is within a few percent. This small splitting results from the combination of two RG effects:

$$m^2_{\tilde{\nu}_\tau} - m^2_{\tilde{\tau}_1} \approx \Delta^{\tilde{\tau}}_{LR}(A_\tau) - c_{\tilde{l}}\cos(2\beta)M_Z^2. \qquad (29)$$

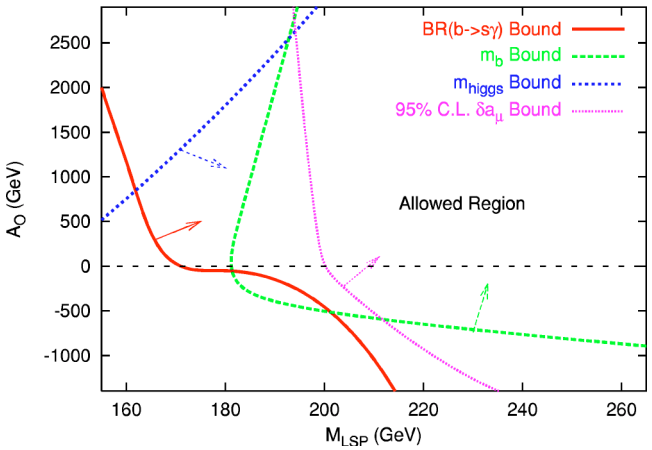

FIG. 13. The determination of the lower bound on $m_{\tilde{\chi}}$ in the case of nonzero A_0, for $\tan\beta=38.0$, $\Delta_{\tilde{b}_1}\simeq 0$, and $K=0.35$. The allowed region is in the upper right part of the figure, as indicated.

The first contribution in Eq. (29) comes from the mixing between $\tilde{\tau}_L$ and $\tilde{\tau}_R$, which depends on A_τ, while the second term stems from the mentioned D-term quartic interaction, and the coefficient $c_{\tilde{l}}\simeq 0.8$ [2]. Even though $A_0=0$ at the GUT scale, RG effects can drive $A_\tau(M_{\rm SUSY})$ to large values (for the case of Fig. 2 we obtain typical values for $A_\tau \approx 0.5$ TeV) and thus entail a nontrivial LR mixing $\Delta^{\tilde{\tau}}_{LR}$. In the case of Fig. 2 we get $m^2_{\tilde{\nu}_\tau} - m^2_{\tilde{\tau}_1} \approx 10$ GeV. In Fig. 14 we plot the cosmophenomenologically allowed region at $K=0.1$ and $\tan\beta=38.0$, in analogy with Fig. 11. We also show the "superconservative" 5σ bound on δa_μ, while the m_b bounds lie outside the depicted range.

Figures 11 and 14 allow us to compare the efficiency of coannihilation processes involving a strongly interacting sparticle (the bottom squark) and a weakly or electromagnetically interacting one (the tau sneutrino and the stau). We see that in the second case the maximum mass splitting between the NLSP and the neutralino is 2%, while in the first one, at the same $m_{\tilde{\chi}}$, the cosmological bound allows a mass splitting up to $\approx 8\%$. In Fig. 15 we plot the allowed regions at $\tan\beta=34$ (a) and 42 (b). We notice in all cases that slepton coannihilations constrain $m_{\tilde{\chi}}$ to less than approximately 0.5 TeV, while in the case of the bottom squark the bound is three times higher.

Remarkably, we see in Figs. 14 and 15 that the 2σ bound on δa_μ coming from τ-decay data is *always satisfied* in the

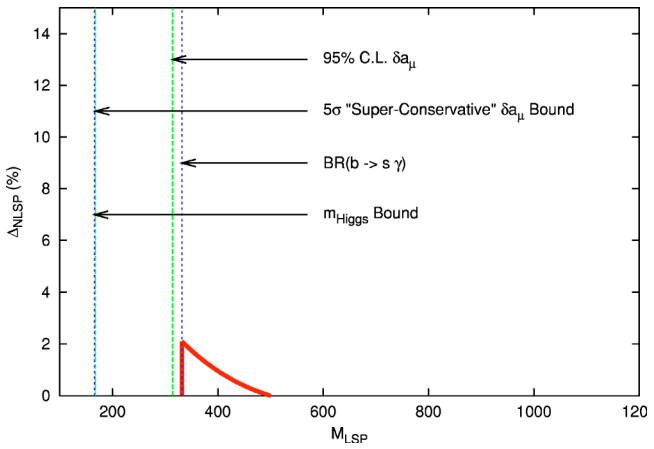

FIG. 14. Cosmologically allowed parameter space in the tau sneutrino–stau coannihilation region, at $K=0.1$ and $\tan\beta=38.0$. The scale of the axis, as well as the notation, are the same as in Fig. 11.

parameter space regions allowed by the other cosmophenomenological constraints.

As regards nonzero values for A_0, we draw in the present case the same conclusions as in the preceding section (see Fig. 13): the type of phenomenological constraint giving the lower bound on $m_{\tilde{\chi}}$ in general changes, but the lowest value of $m_{\tilde{\chi}}$ is determined by the $A_0=0$ case.

The coannihilation pattern is far more complicated in this case than in the bottom squark case. We show in Fig. 16 a typical situation for the (percent) contributions of the possible coannihilating initial sparticles, and a detail of the most relevant final states, taken at $m_{\tilde{\chi}}\simeq m_{\tilde{\nu}_\tau}$ and $\tan\beta=38$. This pattern is, however, rather dependent on the $\tan\beta$ value and on the relative mass splitting. The case of stau–tau sneutrino coannihilation is further discussed in the Appendix.

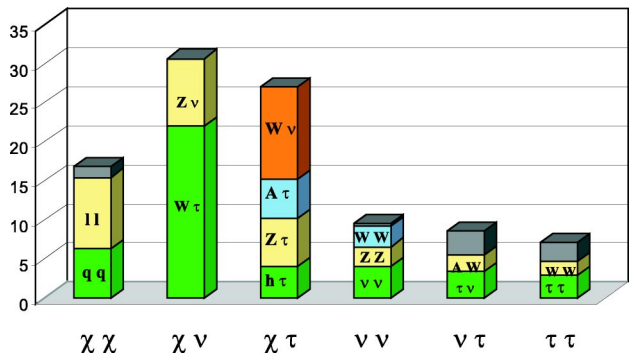

FIG. 16. A typical pattern of the relative contribution's of coannihilation processes in the tau sneutrino coannihilation region. The plot refers to the case $\tan\beta=38$, $A_0=0$, and $m_{\tilde{\chi}}\simeq m_{\tilde{\nu}_\tau}$. The top dark gray parts of the columns represent other contributing channels.

C. The $\tan\beta$ range

From Eq. (16) we notice that the size of the corrections grows (linearly) with $\tan\beta$; therefore we expect that the upper bound on $m_b(M_Z)$ determines the lower bound on $\tan\beta$, and vice versa. As shown by from the figures of Secs. VI A and VI B, the m_b constraint concurs with the other cosmophenomenological bounds, permitting the determination of the allowed range of $\tan\beta$. We determine the lowest limit on $\tan\beta$ by combining the most restrictive phenomenological constraint, which turns out to be BR($b\to s\gamma$) and which gives the lower bound on $m_{\tilde{\chi}}^{\min}\equiv m_{\tilde{\chi}}$, with the upper bound on $m_b^{\rm corr}$, which in its turn gives the upper bound $m_{\tilde{\chi}}^{\max}$. Requiring $m_{\tilde{\chi}}^{\min}=m_{\tilde{\chi}}^{\max}$ unambiguously gives the lowest allowed value of $\tan\beta$. In order to find the upper limit on $\tan\beta$, we notice that the bound on m_b is weaker than the constraint coming from BR($b\to s\gamma$) in determining the low-

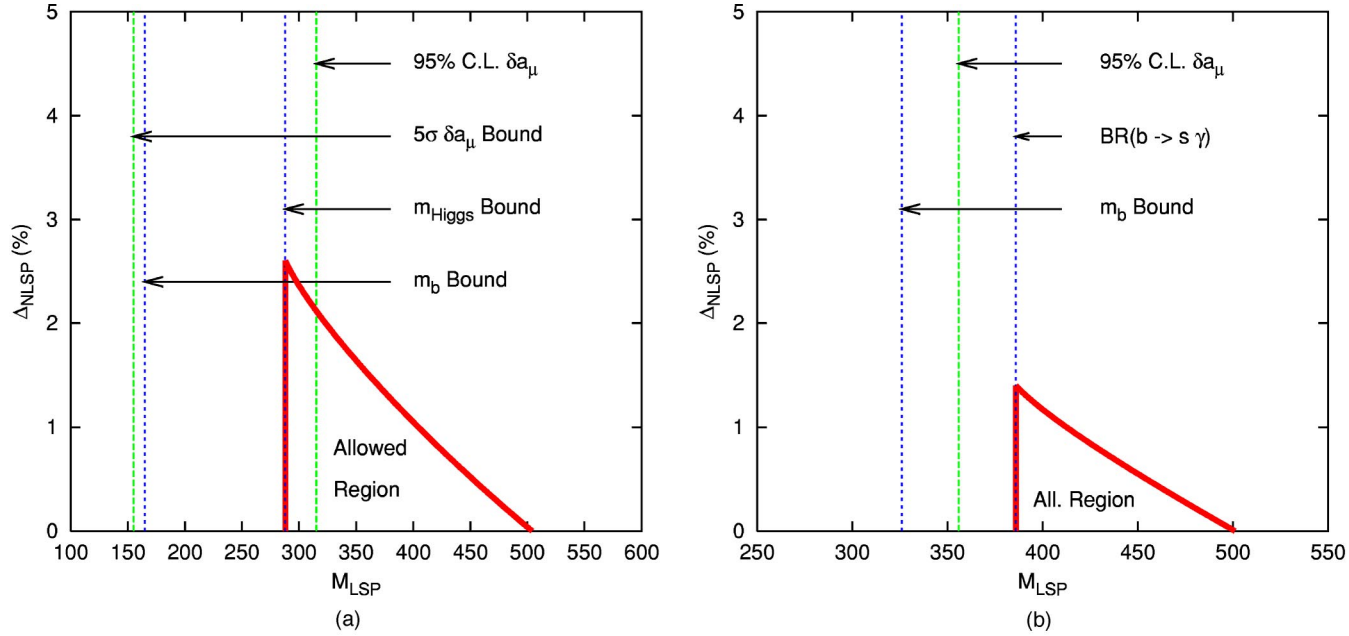

FIG. 15. Cosmophenomenologically allowed parameter space in the tau sneutrino–stau coannihilation region at $K=0.1$ and $\tan\beta=34.0$ (a) and $\tan\beta=42.0$ (b).

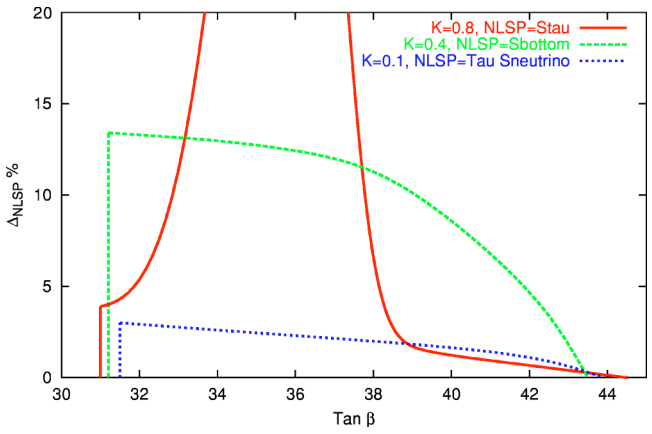

FIG. 17. The allowed $(\tan\beta, \Delta_{\rm NLSP})$ regions for three benchmark K values, $K=0.8,0.4,0.1$, corresponding, respectively, to NLSP$=\tilde{\tau}_1, \tilde{b}_1, \tilde{\nu}_\tau$. Points below the lines are cosmophenomenologically allowed. For $K=0.8$ we find that, for $32 \lesssim \tan\beta \lesssim 38$, the coannihilation region is contiguous to the A-pole direct annihilation region, producing high values for $\Delta_{\rm NLSP}$ which are, however, unrelated to the efficiency of the coannihilation processes.

est value $m_{\tilde{\chi}}^{\rm min}$ [see, e.g., Fig. 12(b) and Fig. 15(b)]. In fact, the BR$(b \to s\gamma)$ constraint becomes more and more stringent as one increases $\tan\beta$. On the other hand, $m_{\tilde{\chi}}^{\rm max}$ is fixed this time by the cosmological constraint on the maximum allowed neutralino relic density [see Sec. V A and Figs. 12(b) and 15(b)]. In Fig. 17 we depict the allowed $\tan\beta$ range in the $(\tan\beta, \Delta_{\rm NLSP})$ plane for three benchmark K values, $K=0.8$, 0.4, and 0.1. Points below the lines are cosmologically and phenomenologically viable. As shown by Fig. 5, in the case of the stau NLSP the coannihilation region can be connected to the A-pole region; hence the allowed $\Delta_{\rm NLSP}$ becomes large and no longer meaningful to test the efficiency of coannihilation processes. Figure 17 also highlights that bottom squark coannihilations allow a larger mass range for the coannihilating particle, since they involve strong interaction processes: the maximum $\Delta_{\rm NLSP}$ extends in this case up to $\approx 13\%$, while in the case of $\tilde{\chi}$-$\tilde{\tau}_1$-$\tilde{\nu}_\tau$ coannihilation its maximum value is around 3%. In the high $\tan\beta$ tail of Fig. 17, as is easily understood, $\tilde{\chi}$-$\tilde{\tau}_1$ coannihilations are slightly less efficient than $\tilde{\chi}$-$\tilde{\tau}_1$-$\tilde{\nu}_\tau$. Although our analysis was limited to benchmark K values, we can conclude from Fig. 17 that in the $\mu<0$ case the allowed $\tan\beta$ range is

$$31 \lesssim \tan\beta \lesssim 45, \quad \mu<0. \tag{30}$$

We checked that the range given in Eq. (30) holds also for $A_0 \neq 0$. We find in fact that in this case an analogous procedure of determination of $(\tan\beta)^{\rm max,min}$ yields weaker limits. What happens at $A_0 \neq 0$ is mainly that the phenomenological bounds tend to push $m_{\tilde{\chi}}^{\rm min,max}$ to higher values; therefore $(\tan\beta)^{\rm max}$ is lowered, while $(\tan\beta)^{\rm min}$ is left substantially unchanged (see, e.g., Fig. 13).

D. Fine-tuning

The question of the quantification of fine-tuning in SUSY models for dark matter, in addition to involving the naturalness of the models, is also related to the possibility of reliably predicting the relic density $\Omega_\chi h^2$ from accelerator measurements of the SUSY input parameters [80]. We emphasize that the present MNUSM models can hardly be regarded as realistic SUSY models, being conceived in order to address the issue of extended sfermion coannihilation processes in the presence of nonuniversal sfermion mass boundary conditions. Nevertheless, it is natural to face here the problem of the fine-tuning related to the extra parameter K appearing in MNUSM models. In fact, as shown by Fig. 1 and Fig. 2, the new coannihilation regions appearing at large m_0 for $K \lesssim 0.5$ are expected to generate abrupt changes in the neutralino relic density for small variations of the MNUSM parameter K. We will follow here the formalism of Ref. [80] in order to study the logarithmic dependence of the neutralino relic density. There, the amount of fine-tuning was described through the overall logarithmic sensitivity

$$\Delta^\Omega \equiv \sqrt{\sum_i \left(\frac{a_i}{\Omega_\chi} \frac{\partial \Omega_\chi}{\partial a_i} \right)^2}, \tag{31}$$

where a_i are generic SUSY input parameters. As outlined in [16], the coannihilation regions tend to have higher fine-tuning due to the steep rise of the cross sections at the onset of coannihilation processes. In the present case we concentrate only on the contribution $\Delta^\Omega(K)$ coming from the parameter K, and study four benchmark cases at fixed $\tan\beta = 38.0$, $M_{1/2}=1100$ GeV, and $A_0=0$. Motivated by Fig. 2, we choose to plot the following values for $(m_0/M_{1/2})$: 0.5, corresponding to the ordinary stau NLSP coannihilation region; 1.6, intersecting the low K sneutrino coannihilation region, where fine-tuning of K is expected to be reasonably low; 2.5 and 4.0, values which cut the steep part of the new coannihilation branch, corresponding, respectively, to tau sneutrino and bottom squark NLSPs, and where fine-tuning is expected to be rather high. Figure 18 reproduces our results: for $(m_0/M_{1/2})=0.5$ and 1.6 we get, as expected, low values for $\Delta^\Omega(K) \lesssim 3$. On the other hand, the sharp onset of coannihilations for $(m_0/M_{1/2})=2.5,4.0$ entails dramatic K fine-tuning peaks, corresponding to values of K such that $m_{\tilde{\chi}} \simeq m_{\tilde{\nu}_\tau}$ and $m_{\tilde{\chi}} \simeq m_{\tilde{b}_1}$, respectively. In the case of the bottom squark, as suggested by Fig. 1, the steepness of $m_{\tilde{b}_1}(K)$ renders the fine-tuning needed to get $m_{\tilde{b}_1} \simeq m_{\tilde{\chi}}$ particularly large.

To conclude, we find that the extended sfermion coannihilation channels of MNUSM models are characterized by a large amount of fine-tuning in the nonuniversality parameter K in the narrow upper part of the coannihilation branch depicted in Fig. 2. Low fine-tuning of K is instead required in the lower part of the branch, at $K \lesssim 0.2$ and $1 \lesssim (m_0/M_{1/2}) \lesssim 2$ and in the standard stau coannihilation strip. Nonetheless, we stress that these scenarios, although motivated in the context of $SU(5)$ SUSY GUTs, are *ad hoc* sketchily simplified, reducing to single parameter K the scalar nonuniversality variables, in order to focus on peculiar coannihilation phenomena. In "realistic" models one could expect to reproduce more naturally, and hence with a smaller amount of fine-tuning, the newly outlined coannihilation regions.

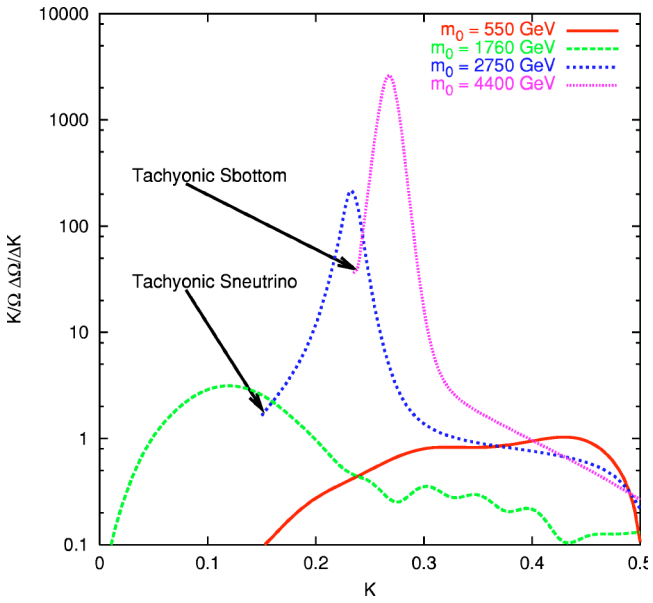

FIG. 18. The fine-tuning parameter $\Delta^{\Omega}(K) \equiv (K/\Omega_{\tilde{\chi}}) \partial \Omega_{\tilde{\chi}} / \partial K$ for the four benchmark values of $m_0 = 550,1760,2750,4400$/GeV. The other SUSY input parameters are fixed at $\tan\beta = 38.0$, $M_{1/2} = 1100$/GeV, and $A_0 = 0$, hence the benchmark m_0 corresponds, respectively, to $(m_0/M_{1/2}) = 0.5,1.6,2.5,4$ (see Fig. 2). At the left end of the lines corresponding to $m_0 = 2750,4400$ the respective NLSP becomes tachyonic, as indicated.

VII. CONCLUSIONS

In this paper we studied the cosmological and phenomenological consequences of top-down b-τ Yukawa coupling unification with minimal nonuniversal boundary conditions in the sfermion masses, inspired by the $SU(5)$ GUT. We showed that the $\mu > 0$ case is ruled out by the b-quark mass bound. We stress that this result holds also in the particular case of full universality (CMSSM). As for the $\mu < 0$ case, b-τ YU is compatible with the set of all known cosmophenomenological constraints, among them the recent results from WMAP, for $31 \lesssim \tan\beta \lesssim 45$. A large parameter space region is also found to be consistent with the 2σ range of δa_μ determined from τ-decay data. Further, if one resorts to a superconservative approach [63] to δa_μ, the whole allowed regions discussed would satisfy the resulting bound.

We found that the SUSY spectrum allows for new types of coannihilation, namely, neutralino–bottom squark and neutralino-tau sneutrino-stau, which we analyzed in detail. We fixed three benchmark scenarios for the three possible coannihilation patterns, including the CMSSM-like case of the neutralino-stau, and we showed for these three cases the behavior of the cosmological and phenomenological constraints as functions of the LSP mass. We then discussed the cosmologically allowed regions for the two types of new coannihilation at various values of $\tan\beta$, and the main channels contributing to the neutralino relic density suppression. An analytical approximate treatment of these channels is given in the Appendix.

ACKNOWLEDGMENTS

I would like to thank S. Bertolini, S. Petcov, P. Ullio, and C. E. Yaguna for many useful discussions, comments, and for support. I also acknowledge C. Pallis for collaboration during the early stages of this work, and A. Djouadi and V. Spanos for helpful remarks.

APPENDIX A: NEUTRALINO RELIC DENSITY CALCULATION IN THE PRESENCE OF COANNIHILATIONS

The starting point to compute the neutralino relic density is the generalization of the Boltzmann equation to a set of N coannihilating species [60,11]:

$$\frac{dn}{dt} = -3Hn - \langle \sigma_{\rm eff} v \rangle (n^2 - n_{\rm eq}^2), \tag{A1}$$

where H is the Hubble constant, $n \equiv \Sigma_{i=1}^{N} n^i$ is the total number density summed over all coannihilating particles, and $n_{\rm eq}$ is the equilibrium number density, which in the Maxwell-Boltzmann approximation, valid in the present cases, reads

$$n_{\rm eq} = \frac{T}{2\pi^2} \sum_{i=1}^{N} g_i m_i^2 K_2\left(\frac{m_i}{T}\right), \tag{A2}$$

g_i being the internal degrees of freedom of particle i of mass m_i, T the photon temperature, and $K_2(x)$ a modified Bessel function. In Eq. (A1) $\sigma_{\rm eff}$ is the effective cross section, defined as

$$\sigma_{\rm eff} = \sum_{i,j=1}^{N} \sigma_{ij} r_i r_j . \tag{A3}$$

In its turn, σ_{ij} is the total cross section for the processes involving ij (co)annihilations, averaged over initial spin and particle-antiparticle states. The coefficients r_i, in the reasonable approximation [11] where the ratio of the number density of species i to the total number density maintains its equilibrium before, during, and after freeze-out, are defined as

$$r_i \equiv \frac{n_{\rm eq}^i}{n_{\rm eq}} = \frac{g_i (1+\Delta_i)^{3/2} e^{-\Delta_i x}}{g_{\rm tot}}, \tag{A4}$$

where

$$g_{\rm tot} = \sum_{i=1}^{N} g_i (1+\Delta_i)^{3/2} e^{-\Delta_i x}, \quad \Delta_i = \frac{m_i - m_{\tilde{\chi}}}{m_{\tilde{\chi}}}, \quad x \equiv \frac{m_{\tilde{\chi}}}{T}. \tag{A5}$$

From Eq. (A4) it is apparent that only species which are quasidegenerate in mass with the LSP can effectively contribute to the coannihilation processes, since large mass differences are exponentially suppressed. Once the freeze-out temperature T_F has been numerically determined, [12] the LSP relic density at the present cosmic time can be evaluated by [11]

$$\Omega_{\tilde{\chi}} h^2 \approx \frac{1.07 \times 10^9 \ \ {\rm GeV}^{-1}}{g_*^{1/2} M_P x_F^{-1} \hat{\sigma}_{\rm eff}}, \tag{A6}$$

TABLE II. Neutralino annihilation and coannihilation with bottom squark, stau, and sneutrino.

Initial state	Final states	Tree level channels
$\tilde{\chi}\tilde{\chi}$	hh, hH, HH, AA, ZZ, AZ,	$s(h)$, $s(H)$, $t(\tilde{\chi}_i^0)$, $u(\tilde{\chi}_i^0)$
	$h[H]A$, $h[H]Z$	$s(A)$, $s(Z)$, $t(\tilde{\chi}_i^0)$, $u(\tilde{\chi}_i^0)$
	W^+W^-, H^+H^-	$s(h)$, $s(H)$, $s(Z)$, $t(\tilde{\chi}_j^-)$, $u(\tilde{\chi}_j^-)$
	$W^\pm H^\pm$	$s(h)$, $s(H)$, $s(A)$, $t(\tilde{\chi}_j^-)$, $u(\tilde{\chi}_j^-)$
	$f\bar{f}$	$s(h)$, $s(H)$, $s(A)$, $s(Z)$, $t(\tilde{f})$, $u(\tilde{f})$
$\tilde{\chi}\tilde{b}_1$	$bh[H]$, bZ	$s(b)$, $t(\tilde{b}_{1,2})$, $u(\tilde{\chi}_i^0)$
	bA	$s(b)$, $t(\tilde{b}_2)$, $u(\tilde{\chi}_i^0)$
	$b\gamma$, bg	$s(b)$, $t(\tilde{b}_1)$
	tH^-, tW^-	$s(b)$, $t(\tilde{t}_{1,2})$, $u(\tilde{\chi}_j^-)$
$\tilde{\chi}\tilde{\tau}_1$	$\tau h[H]$, τZ	$s(\tau)$, $t(\tilde{\tau}_{1,2})$, $u(\tilde{\chi}_i^0)$
	τA	$s(\tau)$, $t(\tilde{\tau}_2)$, $u(\tilde{\chi}_i^0)$
	$\tau\gamma$	$s(\tau)$, $t(\tilde{\tau}_1)$
	$\nu_\tau H^-$, $\nu_\tau W^-$	$s(\tau)$, $t(\tilde{\nu}_\tau)$, $u(\tilde{\chi}_j^-)$
$\tilde{\chi}\tilde{\nu}_\tau$	$\nu_\tau h[H]$, $\nu_\tau Z$	$s(\nu_\tau)$, $t(\tilde{\nu}_\tau)$, $u(\tilde{\chi}_i^0)$
	$\nu_\tau A$	$u(\tilde{\chi}_i^0)$
	τH^+, τW^+	$s(\nu_\tau)$, $t(\tilde{\tau}_{1,2})$, $u(\tilde{\chi}_j^-)$

where $M_P = 1.22 \times 10^{19}$ GeV is the Planck scale, $g_* \approx 81$ is the number of effective degrees of freedom at freeze-out, $x_F = m_{\tilde{\chi}}/T_F$, and

$$\hat{\sigma}_{\rm eff} \equiv x_F \int_{x_F}^{\infty} \langle \sigma_{\rm eff} v \rangle x^{-2} dx \tag{A7}$$

keeps track of the efficiency of post-freeze-out annihilations.

In many cases, one can approximate the thermally averaged product of the relative velocity and the cross section of the (co)annihilating particles through a Taylor expansion,

$$\sigma_{ij} v = a_{ij} + b_{ij} v^2. \tag{A8}$$

This approximation is not accurate near s-channel poles and final-state thresholds, as pointed out in Refs. [11,13]. In all other cases, and in particular in most of those studied in the present paper (an exception is given in Fig. 5), one can proceed and calculate

$$\hat{\sigma}_{\rm eff} = \sum_{i,j} (\alpha_{ij} a_{ij} + \beta_{ij} b_{ij}) \equiv \sum_{ij} \hat{\sigma}_{ij}, \tag{A9}$$

where the sum is extended to all the possible pairs of initial sparticle states, and the coefficients

$$\alpha_{ij} = x_F \int_{x_F}^{\infty} \frac{dx}{x^2} r_i(x) r_j(x), \quad \beta_{ij} = 6 x_F \int_{x_F}^{\infty} \frac{dx}{x^3} r_i(x) r_j(x). \tag{A10}$$

We list in Tables II–V all the possible annihilation and coannihilation processes involving the neutralino, the stau, the bottom squark, and the tau sneutrino. Only a subset of these reactions effectively contributes to the reduction of the neutralino relic density, as described in Secs. VI A and VI B. In particular, in contrast to the case of neutralino annihilation, the largest contributions to Eq. (A9) arising from coannihilation processes come from the a_{ij} coefficients. In Sec. A 2 we give the analytical form of the a_{ij} for the ''new'' coannihilations which arise in the present context of MNUSMs; namely, we study the most relevant processes in the cases of bottom squark–neutralino, bottom squark–bottom squark, and stau–tau sneutrino coannihilations.

A numerical check of the formulas given in Sec. A 2, consisting in a comparison between the computation outlined in this appendix and the numerical results given by MICROMEGAS, confirmed the expected validity of this approximate treatment to a satisfactory extent, in the regimes not affected by the A-pole effects.

1. The coannihilation processes

We report in Tables II–V the complete list of all (co)annihilation processes involving the lightest neutralino, bottom squark, and stau as well as the tau sneutrino. For a given couple of initial sparticles we list both all the possible final states and the tree level channels relative to any final state. c means the four-particle contact interaction, while $s(X)$, $t(X)$, and $u(X)$ mean an s, t, or u channel where X is the exchanged (s)particle. d and u indicate, respectively, the down- and up-type quarks, while l and ν are the charged leptons and the neutrinos of any family, where not differently specified. f stands for a generic fermion (quark or lepton).

TABLE III. Bottom squark annihilations and coannihilations with stau and sneutrino.

Initial state	Final states	Tree level channels
$\tilde{b}_1\tilde{b}_1$	bb	$t(\tilde{\chi}_i^0)$, $u(\tilde{\chi}_i^0)$, $t(\tilde{g})$, $u(\tilde{g})$
$\tilde{b}_1\tilde{b}_1^*$	hh, hH, HH, ZZ	$s(h)$, $s(H)$, $t(\tilde{b}_{1,2})$, $u(\tilde{b}_{1,2})$, c
	AA	$s(h)$, $s(H)$, $t(\tilde{b}_2)$, $u(\tilde{b}_2)$, c
	ZA	$s(h)$, $s(H)$, $t(\tilde{b}_2)$, $u(\tilde{b}_2)$
	$Ah[H]$	$s(Z)$, $t(\tilde{b}_2)$, $u(\tilde{b}_2)$
	$Zh[H]$	$s(Z)$, $t(\tilde{b}_{1,2})$, $u(\tilde{b}_{1,2})$
	W^+W^-, H^+H^-	$s(h)$, $s(H)$, $s(Z)$, $t(\tilde{t}_{1,2})$, c, $s(\gamma)$
	$W^\pm H^\mp$	$s(h)$, $s(H)$, $t(\tilde{t}_{1,2})$
	$t\bar{t}$, $u\bar{u}$	$s(h)$, $s(H)$, $s(Z)$, $s(\gamma)$, $s(g)$, $t(\tilde{\chi}_j^-)$
	$b\bar{b}$	$s(h)$, $s(H)$, $s(Z)$, $s(\gamma)$, $s(g)$, $t(\tilde{\chi}_j^-)$, $t(\tilde{g})$
	$d\bar{d}$	$s(h)$, $s(H)$, $s(Z)$, $s(\gamma)$, $s(g)$
	$l\bar{l}$	$s(h)$, $s(H)$, $s(Z)$, $s(\gamma)$
	$\nu\bar{\nu}$	$s(Z)$
	$\gamma\gamma$, γZ, γg, Zg	$t(\tilde{b}_1)$, $u(\tilde{b}_1)$, c
	$\gamma h[H]$, $gh[H]$	$t(\tilde{b}_1)$, $u(\tilde{b}_1)$
	gg	$s(g)$, $t(\tilde{b}_1)$, $u(\tilde{b}_1)$, c
$\tilde{b}_1\tilde{\tau}_1$	$b\tau$	$t(\tilde{\chi}_i^0)$
$\tilde{b}_1\tilde{\tau}_1^*$	$b\bar{\tau}$	$t(\tilde{\chi}_i^0)$
	$t\bar{\nu}_\tau$	$t(\tilde{\chi}_j^-)$
$\tilde{b}_1\tilde{\nu}_\tau$	$b\nu_\tau$	$t(\tilde{\chi}_i^0)$
	$t\tau$	$t(\tilde{\chi}_j^-)$
$\tilde{b}_1\tilde{\nu}_\tau^*$	$b\bar{\nu}_\tau$	$t(\tilde{\chi}_i^0)$

2. Relevant approximate formulas for the relic density calculation in the coannihilation regions

The a coefficients for the pair annihilation of neutralinos can be readily and completely derived from Ref. [81], while those concerning the stau annihilations and coannihilations can be calculated from the formulas of Refs. [82] and [15,42]. Some instances of a-coefficient computations can be found in Ref. [17], with the corrections given in [70]. We follow here the notation set in [17]. As regards the tau sneutrino (co)annihilations, the relative a coefficients can be readily derived from those of the stau via suitable replacements in the couplings (e.g., $g_{\tilde{\tau}_1\tilde{\tau}_1 h} \to g_{\tilde{\nu}_\tau\tilde{\nu}_\tau h}$, etc.), in the masses of the (s)particles (e.g. $m_{\tilde{\tau}_1} \to m_{\tilde{\nu}_\tau}$), and by setting the mixing angle between the stau mass eigenstates to zero. We do not give any explicit formulas for the bottom squark–stau and the bottom squark–sneutrino coannihilations, since even in the transition regions where $m_{\tilde{b}_1} \simeq m_{\tilde{\nu}_\tau} \simeq m_{\tilde{\tau}_1}$ these processes do not give any sizable contribution to the neutralino relic density suppression (namely, their total contribution is always less than 0.5%). Therefore we are left with the "new" (co)annihilation processes involving, respectively, *neutralino–bottom squark*, *bottom squark–bottom squark*, and *stau–tau sneutrino*.

We give here the explicit formulas for the dominant processes, as discussed in Secs. VI A and VI B. In the kinematic part of the a coefficients we neglect the mass of the final standard model particles up to and including the b quark. Since the mass of the final SM particles $m_{\rm SM}$ appears there as $m_{\rm SM}^2/m_{\rm SUSY}^2$, the corrections are in fact always negligible. On the other hand, we keep track of both m_b and m_τ if the couplings or the whole amplitudes are proportional to them, as is the case in some of the considered processes. Moreover, in the processes involving the bottom squark we followed the approximations of Ref. [18], neglecting the terms in $\alpha_{\rm e.m.}$ and α_W. A bar over a mass means that the mass is divided by the sum of the masses of the incoming sparticles. S stands for the three neutral physical Higgs bosons h, H, and A, and m_S for the respective masses, $s_X \equiv \sin\theta_X$, $c_X \equiv \cos\theta_X$, and for the other symbols we follow the notation of Ref. [3].

TABLE IV. Stau annihilations and coannihilations with sneutrino.

Initial state	Final states	Tree level channels
$\tilde{\tau}_1\tilde{\tau}_1$	$\tau\tau$	$t(\tilde{\chi}_i^0)$, $u(\tilde{\chi}_i^0)$
$\tilde{\tau}_1\tilde{\tau}_1^*$	hh, hH, HH, ZZ	$s(h)$, $s(H)$, $t(\tilde{\tau}_{1,2})$, $u(\tilde{\tau}_{1,2})$, c
	AA	$s(h)$, $s(H)$, $t(\tilde{\tau}_2)$, $u(\tilde{\tau}_2)$, c
	AZ	$s(h)$, $s(H)$, $t(\tilde{\tau}_2)$, $u(\tilde{\tau}_2)$
	$Ah[H]$	$s(Z)$, $t(\tilde{\tau}_2)$, $u(\tilde{\tau}_2)$
	$Zh[H]$	$s(Z)$, $t(\tilde{\tau}_{1,2})$, $u(\tilde{\tau}_{1,2})$
	W^+W^-, H^+H^-	$s(h)$, $s(H)$, $s(Z)$, $u(\tilde{\nu}_\tau)$, c, $s(\gamma)$
	$W^\pm H^\mp$	$s(h)$, $s(H)$, $u(\tilde{\nu}_\tau)$
	$u\bar{u}$, $d\bar{d}$, $l\bar{l}$	$s(h)$, $s(H)$, $s(Z)$, $s(\gamma)$
	$\tau\bar{\tau}$	$s(h)$, $s(H)$, $s(Z)$, $t(\tilde{\chi}_i^0)$, $s(\gamma)$
	$\nu_\tau\bar{\nu}_\tau$	$s(Z)$, $t(\tilde{\chi}_j^-)$
	$\nu\bar{\nu}$	$s(Z)$
	$\gamma\gamma$, γZ	c, $t(\tilde{\tau}_1)$, $u(\tilde{\tau}_1)$
	$\gamma h[H]$	$t(\tilde{\tau}_1)$, $u(\tilde{\tau}_1)$
$\tilde{\tau}_1\tilde{\nu}_\tau$	$\nu_\tau\tau$	$t(\tilde{\chi}_i^0)$, $u(\tilde{\chi}_j^-)$
$\tilde{\tau}_1\tilde{\nu}_\tau^*$	$\bar{u}d$, $\bar{\nu}l$	$s(H^-)$, $s(W^-)$
	$\bar{\nu}_\tau\tau$	$s(W^-)$, $s(H^-)$, $t(\tilde{\chi}_i^0)$
	ZW^-	$s(W^-)$, $u(\tilde{\tau}_{1,2})$, $t(\tilde{\nu}_\tau)$, c
	γW^-	$s(W^-)$, $u(\tilde{\tau}_1)$, c
	ZH^-	$s(H^-)$, $u(\tilde{\tau}_{1,2})$, $t(\tilde{\nu}_\tau)$
	γH^-	$s(H^-)$, $u(\tilde{\tau}_1)$
	W^-h, W^-H	$s(H^-)$, $s(W^-)$, $u(\tilde{\tau}_{1,2})$, $t(\tilde{\nu}_\tau)$
	W^-A	$s(H^-)$, $u(\tilde{\tau}_2)$
	H^-h, H^-H	$s(H^-)$, $s(W^-)$, $u(\tilde{\tau}_{1,2})$, $t(\tilde{\nu}_\tau)$, c
	H^-A	$s(W^-)$, $u(\tilde{\tau}_2)$, c

TABLE V. Sneutrino annihilations.

Initial state	Final states	Tree level channels
$\tilde{\nu}_\tau\tilde{\nu}_\tau$	$\nu_\tau\nu_\tau$	$t(\tilde{\chi}_i^0)$, $u(\tilde{\chi}_i^0)$
$\tilde{\nu}_\tau\tilde{\nu}_\tau^*$	hh, hH, HH, ZZ	$s(h)$, $s(H)$, $t(\tilde{\nu}_\tau)$, $u(\tilde{\nu}_\tau)$, c
	AA	$s(h)$, $s(H)$, c
	ZA	$s(h)$, $s(H)$
	$Zh[H]$	$s(Z)$, $t(\tilde{\nu}_\tau)$, $u(\tilde{\nu}_\tau)$
	W^+W^-, H^+H^-	$s(h)$, $s(H)$, $s(Z)$, $t(\tilde{\tau}_{1,2})$, c
	$W^\pm H^\mp$	$s(h)$, $s(H)$, $t(\tilde{\tau}_{1,2})$
	$u\bar{u}$, $d\bar{d}$, $l\bar{l}$,	$s(h)$, $s(H)$, $s(Z)$
	$\tau\bar{\tau}$	$s(h)$, $s(H)$, $s(Z)$, $t(\tilde{\chi}_i^0)$
	$\nu_\tau\bar{\nu}_\tau$	$s(Z)$, $t(\tilde{\chi}_i^0)$
	$Ah[H]$, $\nu\bar{\nu}$	$s(Z)$

TABLE VI. Relevant couplings used in the formulas of Secs. A 2(b)–2(d) (part I).

g symbol	Expression
$g^L_{\tilde{b}_1 b\tilde{\chi}_i}$	$\frac{-g_2}{\sqrt{2}}\left[c_{\tilde{b}}\left(N_{i2}-\frac{\tan\theta_W}{6}N_{i1}\right)+s_{\tilde{b}}\frac{m_b N_{i3}}{m_W\cos\beta}\right]$
$g^R_{\tilde{b}_1 b\tilde{\chi}_i}$	$\frac{-g_2}{\sqrt{2}}\left(c_{\tilde{b}}\frac{m_b N_{i3}}{m_W\cos\beta}+\frac{2}{3}s_{\tilde{b}}\tan\theta_W N_{i1}\right)\mathrm{sgn}(m_{\tilde{\chi}^0_i})$
$g_{\tilde{b}_1\tilde{b}_1 g}=g_{bbg}=g_{ggg}$	$-g_s$
$g^L_{\tilde{b}_1 bg}$	$\sqrt{2}g_s s_{\tilde{b}}$
$g^R_{\tilde{b}_1 bg}$	$-\sqrt{2}g_s c_{\tilde{b}}$
$g^{\oplus}_{\tilde{b}_1 b\tilde{\chi}_i}$	$\frac{1}{2}(g^L_{\tilde{b}_1 b\tilde{\chi}_i}+g^R_{\tilde{b}_1 b\tilde{\chi}_i})$
$g^{\ominus}_{\tilde{b}_1 b\tilde{\chi}_i}$	$\frac{1}{2}(g^L_{\tilde{b}_1 b\tilde{\chi}_i}-g^R_{\tilde{b}_1 b\tilde{\chi}_i})$
$g_{\tilde{b}_1\tilde{b}_1 gg}$	g_s^2
$g_{h[H]\tilde{\tau}_1\tilde{\tau}_1}$	$-\frac{g_2}{2c_W}m_Z s_{\alpha+\beta}[-c_{\alpha+\beta}]((1-2s_W^2)s_{\tilde{\tau}}^2+2s_W^2 c_{\tilde{\tau}}^2)$
	$+\frac{g_2 m_\tau}{M_W c_\beta}[m_\tau s_\alpha[-c_\alpha]+s_{\tilde{\tau}}c_{\tilde{\tau}}(A_\tau s_\alpha[-c_\alpha]+\mu c_\alpha[s_\alpha])]$
$g_{A\tilde{\tau}_1\tilde{\tau}_1}$	0
$g_{W\tilde{\nu}_\tau\tilde{\tau}_1}$	$\frac{g_2 s_{\tilde{\tau}}}{\sqrt{2}}$
$g_{W\tilde{\nu}_\tau\tilde{\tau}_2}$	$-\frac{g_2 c_{\tilde{\tau}}}{\sqrt{2}}$
$g_{H^+h[H]W^-}$	$-\frac{g_2}{2}c_{\alpha-\beta}[s_{\alpha-\beta}]$
$g_{H^+AW^-}$	$\frac{g_2}{2}$
$g_{H^+\tilde{\nu}_\tau\tilde{\tau}_1}$	$\frac{g_2 M_W s_{\tilde{\tau}}}{\sqrt{2}}s_{2\beta}$

a. Couplings

The couplings are given in Tables VI and VII.

b. $\tilde{\chi}$-$\tilde{b}_1$ coannihilations

$\tilde{\chi}\tilde{b}_1\to bg$:

$$\frac{1}{24\pi m^2_{\tilde{b}_1}}\{(g^L_{\tilde{b}_1 b\tilde{\chi}_1}+g^R_{\tilde{b}_1 b\tilde{\chi}_1})[g^2_{\tilde{b}_1\tilde{b}_1 g}(\overline{m}_{\tilde{\chi}^0_1}-\overline{m}_{\tilde{b}_1})+g^2_{bbg}\overline{m}_{\tilde{b}_1}]-4g_{bbg}g_{\tilde{b}_1\tilde{b}_1 g}[(g^L_{\tilde{b}_1 b\tilde{\chi}_1})^2+(g^R_{\tilde{b}_1 b\tilde{\chi}_1})^2](\overline{m}_{\tilde{\chi}^0_1}-\overline{m}_{\tilde{b}_1})\}.$$

c. $\tilde{b}_1$-$\tilde{b}_1$ annihilations

$\tilde{b}_1\tilde{b}_1\to bb$:

$$\frac{[(g^L_{\tilde{b}_1 bg})^2+(g^R_{\tilde{b}_1 bg})^2]m^2_{\tilde{g}}+g^L_{\tilde{b}_1 bg}g^R_{\tilde{b}_1 bg}m^2_{\tilde{b}_1}}{54\pi(m^2_{\tilde{g}}+m^2_{\tilde{b}_1})^2}+\sum_{i,j=1}^{4}\left\{\frac{m_{\tilde{\chi}_i}m_{\tilde{\chi}_j}[(g^{\oplus}_{\tilde{b}_1 b\tilde{\chi}_i})^2+(g^{\ominus}_{\tilde{b}_1 b\tilde{\chi}_i})^2][(g^{\oplus}_{\tilde{b}_1 b\tilde{\chi}_j})^2+(g^{\ominus}_{\tilde{b}_1 b\tilde{\chi}_j})^2]}{2\pi(m^2_{\tilde{\chi}_i}+m^2_{\tilde{b}_1})(m^2_{\tilde{\chi}_j}+m^2_{\tilde{b}_1})}\right.$$

$$\left.+\frac{4m_{\tilde{\chi}_i}m_{\tilde{\chi}_j}g^{\oplus}_{\tilde{b}_1 b\tilde{\chi}_i}g^{\ominus}_{\tilde{b}_1 b\tilde{\chi}_i}g^{\oplus}_{\tilde{b}_1 b\tilde{\chi}_j}g^{\ominus}_{\tilde{b}_1 b\tilde{\chi}_j}+m^2_{\tilde{b}_1}(g^{\oplus}_{\tilde{b}_1 b\tilde{\chi}_i})^2(g^{\ominus}_{\tilde{b}_1 b\tilde{\chi}_j})^2}{4\pi(m^2_{\tilde{\chi}_i}+m^2_{\tilde{b}_1})(m^2_{\tilde{\chi}_j}+m^2_{\tilde{b}_1})}\right\}.$$

TABLE VII. Relevant couplings used in the formulas of Secs. A 2(b)–2(d) (part II).

g symbol	Expression
$g_{h[H]W^+W^-}$	$g_2 M_W s_{\beta-\alpha}[c_{\beta-\alpha}]$
$g_{AW^+W^-}$	0
$g_{h[H]\tilde{\tau}_1\tilde{\tau}_2}$	$\frac{g_2}{2c_W} m_Z s_{\alpha+\beta}[-c_{\alpha+\beta}](1-4s_W^2) s_{\tilde{\tau}} c_{\tilde{\tau}} + g_2 m_\tau (c_{\tilde{\tau}}^2 - s_{\tilde{\tau}}^2) \frac{A_\tau s_\alpha[-c_\alpha] + \mu c_\alpha[s_\alpha]}{2M_W c_\beta}$
$g_{A\tilde{\tau}_1\tilde{\tau}_2}$	$g_2 m_\tau \frac{A_\tau \tan\beta + \mu}{2M_W}$
$g_{WZ\tilde{\nu}_\tau\tilde{\tau}_1}$	$\frac{g_2^2 s_W^2}{\sqrt{2} c_W} s_{\tilde{\tau}}$
g_{WWZ}	$g_2 c_W$
g_{Wtb}	$-\frac{g_2}{\sqrt{2}}$
$g^L_{H^+tb}$	$\frac{g_2}{\sqrt{2}M_W}(m_t \cot\beta)$
$g^R_{H^+tb}$	$\frac{g_2}{\sqrt{2}M_W}(m_b \tan\beta)$
$g^L_{\tilde{\tau}_1\tau\tilde{\chi}_i^0}$	$s_{\tilde{\tau}} \frac{g_2}{\sqrt{2}M_W} \frac{N_{i3}^* m_\tau}{c_\beta} + c_{\tilde{\tau}} \left(\frac{\sqrt{2} g_2}{c_W} s_W^2 N_{i2}'^* - \sqrt{2} g_1 c_W N_{i1}'^* \right)$
$g^R_{\tilde{\tau}_1\tau\tilde{\chi}_i^0}$	$-s_{\tilde{\tau}} \sqrt{2} \left[g_1 c_W N_{i1}' + \frac{g_2}{c_W} (\frac{1}{2} - s_W^2) N_{i2}' \right] - c_{\tilde{\tau}} \frac{g_2}{\sqrt{2}M_W} \frac{N_{i3} m_\tau}{c_\beta}$
$g^L_{\tilde{\nu}_\tau\nu_\tau\tilde{\chi}_i^0}$	0
$g^R_{\tilde{\nu}_\tau\nu_\tau\tilde{\chi}_i^0}$	$-\frac{g_2}{\sqrt{2}M_W} N_{i2}'$
$g^L_{\tilde{\tau}_1\nu_\tau\tilde{\chi}_j^-}$	$\frac{g_2}{\sqrt{2}M_W} \frac{U_{j2} m_\tau}{c_\beta} c_{\tilde{\tau}}$
$g^R_{\tilde{\tau}_1\nu_\tau\tilde{\chi}_j^-}$	$g_2 U_{j1} s_{\tilde{\tau}}$
$g^L_{\tilde{\nu}_\tau\tau\tilde{\chi}_j^-}$	$\frac{g_2}{\sqrt{2}M_W} \frac{U_{j2}^* m_\tau}{c_\beta}$
$g^R_{\tilde{\nu}_\tau\tau\tilde{\chi}_j^-}$	$-g_2 V_{j1}$

$\tilde{b}_1\tilde{b}_1^* \to gg$:

$$\frac{81 g_{ggg}^2 g_{\tilde{b}_1\tilde{b}_1 g}^2 + 56 g_{\tilde{b}_1\tilde{b}_1 gg}(2 g_{\tilde{b}_1\tilde{b}_1 gg} - g_{\tilde{b}_1\tilde{b}_1 g})}{1728\pi m_{\tilde{b}_1}^2}.$$

d. $\tilde{\tau}_1$-$\tilde{\nu}_\tau$ coannihilations

$\tilde{\nu}_\tau\tilde{\tau}_2^* \to SW^+$:

$$\frac{\{[1-(\bar{M}_W+\bar{m}_S)^2][1-(\bar{M}_W-\bar{m}_S)^2]\}^{3/2}}{128\pi M_W^2 m_{\tilde{\nu}_\tau} m_{\tilde{\tau}_1}} \left[\frac{2 g_{S\tilde{\tau}_1\tilde{\tau}_1} g_{W\tilde{\nu}_\tau\tilde{\tau}_1} m_{\tilde{\nu}_\tau}}{m_{\tilde{\nu}_\tau}\bar{m}_S^2 - m_{\tilde{\tau}_1}(1-\bar{M}_W^2)} + \frac{2 g_{H^+SW^-} g_{H^+\tilde{\nu}_\tau\tilde{\tau}_1} \bar{m}_{\tilde{\nu}_\tau}}{1-\bar{m}_{H^\pm}^2} \right.$$
$$\left. + \frac{g_{W\tilde{\nu}_\tau\tilde{\tau}_1} g_{SW^+W^-}[(\bar{m}_{\tilde{\nu}_\tau} - \bar{m}_{\tilde{\tau}_1})^2 - \bar{M}_W^2]}{\bar{M}_W^2(1-\bar{M}_W^2)} + \frac{2 g_{S\tilde{\tau}_1\tilde{\tau}_2} g_{W\tilde{\nu}_\tau\tilde{\tau}_2} m_{\tilde{\nu}_\tau}}{m_{\tilde{\nu}_\tau}\bar{m}_S^2 - \bar{m}_{\tilde{\nu}_\tau}^2 m_{\tilde{\tau}_1} - m_{\tilde{\nu}_\tau}(\bar{m}_{\tilde{\tau}_2}^2 + \bar{m}_{\tilde{\tau}_1}^2) - m_{\tilde{\tau}_1}(\bar{m}_{\tilde{\tau}_2}^2 - \bar{M}_W^2)} \right]^2.$$

$\tilde{\nu}_\tau \tilde{\tau}_2^* \to ZW^+$:

$$\frac{\{[1-(\bar{M}_W+\bar{M}_Z)^2][1-(\bar{M}_W-\bar{M}_Z)^2]\}^{1/2}}{32\pi m_{\tilde{\nu}_\tau} m_{\tilde{\tau}_2}}\left[\left(\frac{\bar{M}_W^2+\bar{M}_Z^2-1}{2\bar{M}_Z\bar{M}_W}\right)^2+2\right]\left[7g^2_{WZ\tilde{\nu}_\tau\tilde{\tau}_1}+7g^2_{W\tilde{\nu}_\tau\tilde{\tau}_1}g^2_{WWZ}\left(1-\frac{M_Z^2}{M_W^2}\right)\right.$$
$$\left.+4g_{WZ\tilde{\nu}_\tau\tilde{\tau}_1}g_{W\tilde{\nu}_\tau\tilde{\tau}_1}g_{WWZ}\left(1-\frac{M_Z^2}{M_W^2}\right)^2\right].$$

$\tilde{\nu}_\tau \tilde{\tau}_2^* \to b\bar{t}$:

$$\frac{(1-\bar{m}_t^2)^2}{16\pi m_{\tilde{\nu}_\tau} m_{\tilde{\tau}_1}}\left[g^2_{W\tilde{\nu}_\tau\tilde{\tau}_1}g^2_{Wtb}\frac{\bar{m}_b\bar{m}_t}{\bar{M}_W^4}+\frac{\bar{g}^2_{H^+\tilde{\nu}_\tau\tilde{\tau}_1}}{(1-\bar{m}^2_{H^\pm})^2}\{[|g^L_{H^+tb}|^2+|g^R_{H^+tb}|^2]\bar{m}_b\bar{m}_t+(g^L_{H^+tb}g^R_{H^+tb})(\bar{m}_t^2-1)\}\right.$$
$$\left.+\frac{\bar{g}_{H^+\tilde{\nu}_\tau\tilde{\tau}_1}g_{W\tilde{\nu}_\tau\tilde{\tau}_1}g_{Wtb}}{\bar{M}_W^2(1-\bar{m}^2_{H^\pm})}[g^L_{H^+tb}\bar{m}_t(1-\bar{m}_t^2)-g^R_{H^+tb}\bar{m}_b(1+\bar{m}_t^2)]\right].$$

$\tilde{\nu}_\tau \tilde{\tau}_2 \to \nu_\tau \tau$:

$$\left(\frac{m_\tau^2}{32\pi m_{\tilde{\nu}_\tau} m_{\tilde{\tau}_1}}\right)\left\{\sum_{i,k=1}^{4}\frac{m^2_{\tilde{\nu}_\tau}\mathrm{Re}[g^L_{\tilde{\tau}_1\tau\tilde{\chi}^0_i}(g^L_{\tilde{\tau}_1\tau\tilde{\chi}^0_k})^* g^R_{\tilde{\nu}_\tau\nu_\tau\tilde{\chi}^0_i}(g^R_{\tilde{\nu}_\tau\nu_\tau\tilde{\chi}^0_k})^*]}{(m^2_{\tilde{\chi}^0_i}+m_{\tilde{\nu}_\tau}m_{\tilde{\tau}_1})(m^2_{\tilde{\chi}^0_k}+m_{\tilde{\nu}_\tau}m_{\tilde{\tau}_1})}+\sum_{i,k=1}^{4}\frac{m^2_{\tilde{\nu}_\tau}\mathrm{Re}[g^L_{\tilde{\nu}_\tau\nu_\tau\tilde{\chi}^0_i}(g^L_{\tilde{\nu}_\tau\nu_\tau\tilde{\chi}^0_k})^* g^R_{\tilde{\tau}_1\tau\tilde{\chi}^0_i}(g^R_{\tilde{\tau}_1\tau\tilde{\chi}^0_k})^*]}{(m^2_{\tilde{\chi}^0_i}+m_{\tilde{\nu}_\tau}m_{\tilde{\tau}_1})(m^2_{\tilde{\chi}^0_k}+m_{\tilde{\nu}_\tau}m_{\tilde{\tau}_1})}\right.$$
$$+\sum_{j,l=1}^{2}\frac{m^2_{\tilde{\tau}_1}\mathrm{Re}[g^L_{\tilde{\tau}_1\nu_\tau\tilde{\chi}^-_j}(g^L_{\tilde{\tau}_1\nu_\tau\tilde{\chi}^-_l})^* g^R_{\tilde{\nu}_\tau\tau\tilde{\chi}^-_j}(g^R_{\tilde{\nu}_\tau\tau\tilde{\chi}^-_l})^*]}{(m^2_{\tilde{\chi}^-_j}+m_{\tilde{\nu}_\tau}m_{\tilde{\tau}_1})(m^2_{\tilde{\chi}^-_l}+m_{\tilde{\nu}_\tau}m_{\tilde{\tau}_1})}+\sum_{j,l=1}^{2}\frac{m^2_{\tilde{\tau}_1}\mathrm{Re}[g^L_{\tilde{\nu}_\tau\tau\tilde{\chi}^-_j}(g^L_{\tilde{\nu}_\tau\tau\tilde{\chi}^-_l})^* g^R_{\tilde{\tau}_1\nu_\tau\tilde{\chi}^-_j}(g^R_{\tilde{\tau}_1\nu_\tau\tilde{\chi}^-_l})^*]}{(m^2_{\tilde{\chi}^-_j}+m_{\tilde{\nu}_\tau}m_{\tilde{\tau}_1})(m^2_{\tilde{\chi}^-_l}+m_{\tilde{\nu}_\tau}m_{\tilde{\tau}_1})}$$
$$\left.-\sum_{i=1}^{4}\sum_{j=1}^{2}\frac{m_{\tilde{\tau}_1}m_{\tilde{\nu}_\tau}\mathrm{Re}[(g^L_{\tilde{\nu}_\tau\tau\tilde{\chi}^-_j})^* g^L_{\tilde{\tau}_1\tau\tilde{\chi}^0_i}g^R_{\tilde{\nu}_\tau\nu_\tau\tilde{\chi}^0_i}(g^R_{\tilde{\tau}_1\nu_\tau\tilde{\chi}^-_j})^*]}{(m^2_{\tilde{\chi}^0_i}+m_{\tilde{\nu}_\tau}m_{\tilde{\tau}_1})(m^2_{\tilde{\chi}^-_j}+m_{\tilde{\nu}_\tau}m_{\tilde{\tau}_1})}-\sum_{i=1}^{4}\sum_{j=1}^{2}\frac{m_{\tilde{\tau}_1}m_{\tilde{\nu}_\tau}\mathrm{Re}[g^L_{\tilde{\nu}_\tau\nu_\tau\tilde{\chi}^0_i}(g^L_{\tilde{\tau}_1\nu_\tau\tilde{\chi}^-_j})^*(g^R_{\tilde{\nu}_\tau\tau\tilde{\chi}^-_j})^* g^R_{\tilde{\tau}_1\tau\tilde{\chi}^0_i}]}{(m^2_{\tilde{\chi}^0_i}+m_{\tilde{\nu}_\tau}m_{\tilde{\tau}_1})(m^2_{\tilde{\chi}^-_j}+m_{\tilde{\nu}_\tau}m_{\tilde{\tau}_1})}\right\}.$$

[1] For a review on grand unified theories, see, e.g., P. Langacker, Phys. Rep. **72**, 185 (1981).

[2] For a review on SUSY GUTs, see, e.g., W. de Boer, Prog. Part. Nucl. Phys. **33**, 201 (1994).

[3] H.E. Haber and G.L. Kane, Phys. Rep. **117**, 76 (1985); J.F. Gunion and H.E. Haber, Nucl. Phys. **B272**, 1 (1986).

[4] A. Chamseddine, R. Arnowitt, and P. Nath, Phys. Rev. Lett. **49**, 970 (1982); R. Barbieri, S. Ferrara, and C. Savoy, Phys. Lett. **119B**, 343 (1982); L.J. Hall, J. Lykken, and S. Weinberg, Phys. Rev. D **27**, 2359 (1983).

[5] S. Profumo, Talk given at the XXXVIIIth Rencontres de Moriond on ElectroWeak Interactions and Unified Theories, 2003, to appear in the Proceedings.

[6] For a review, see, e.g., G. Jungman, M. Kamionkowski, and K. Griest, Phys. Rep. **267**, 195 (1996).

[7] D.N. Spergel *et al.*, astro-ph/0302209.

[8] J. Ellis, K.A. Olive, Y. Santoso, and V.C. Spanos, hep-ph/0303043.

[9] H. Baer and C. Balazs, hep-ph/0303114; A.B. Lahanas and D.V. Nanopoulos, hep-ph/0303130.

[10] P. Salati, astro-ph/0207396.

[11] K. Griest and D. Seckel, Phys. Rev. D **43**, 3191 (1991).

[12] K. Griest, M. Kamionkowski, and M.S. Turner, Phys. Rev. D **41**, 3565 (1990).

[13] P. Gondolo and G. Gelmini, Nucl. Phys. **B360**, 145 (1991).

[14] A. Djouadi, M. Drees, and J.L. Kneur, J. High Energy Phys. **08**, 055 (2001).

[15] J. Ellis, T. Falk, K.A. Olive, and M. Srednicki, Astropart. Phys. **13**, 181 (2000); **15**, 413(E) (2001).

[16] H. Baer, C. Balazs, and A. Belyaev, J. High Energy Phys. **03**, 042 (2002).

[17] M.E. Gomez, G. Lazarides, and C. Pallis, Phys. Rev. D **61**, 123512 (2000).

[18] J. Ellis, K.A. Olive, and Y. Santoso, Astropart. Phys. **18**, 395 (2003).

[19] C. Boehm, A. Djouadi, and M. Drees, Phys. Rev. D **62**, 035012 (2000).

[20] J. Edsjo, M. Schelke, P. Ullio, and P. Gondolo, J. Cosmol. Astropart. Phys. **04**, 001 (2003).

[21] B. Ananthanarayan, G. Lazarides, and Q. Shafi, Phys. Rev. D **44**, 1613 (1991); Phys. Lett. B **300**, 245 (1993); G. Anderson *et al.*, Phys. Rev. D **47**, 3702 (1993); **49**, 3660 (1994); V. Barger, M. Berger, and P. Ohmann, *ibid.* **49**, 4908 (1994); B. Ananthanarayan, Q. Shafi, and X. Wang, *ibid.* **50**, 5980 (1994);

R. Rattazzi and U. Sarid, *ibid.* **53**, 1553 (1996).
[22] M. Carena, M. Olechowski, S. Pokorski, and C.E. Wagner, Nucl. Phys. **B426**, 269 (1994).
[23] H. Baer, M.A. Diaz, J. Ferrandis, and X. Tata, Phys. Rev. D **61**, 111701 (2000); H. Baer, M. Brhlik, M.A. Diaz, J. Ferrandis, P. Mercadante, P. Quintana, and X. Tata, *ibid.* **63**, 015007 (2001); H. Baer and J. Ferrandis, Phys. Rev. Lett. **87**, 211803 (2001); D. Auto, H. Baer, C. Balazs, A. Belyaev, J. Ferrandis, and X. Tata, hep-ph/0302155; R. Dermisek, S. Raby, L. Roszkowski, and R. Ruiz de Austri, J. High Energy Phys. **04**, 037 (2003).
[24] L.J. Hall, R. Rattazzi, and U. Sarid, Phys. Rev. D **50**, 7048 (1994); R. Hempfling, *ibid.* **49**, 6168 (1994).
[25] M.S. Chanowitz, J. Ellis, and M.K. Gaillard, Nucl. Phys. **B128**, 506 (1977); A.J. Buras, J. Ellis, M.K. Gaillard, and D.V. Nanopolous, *ibid.* **B135**, 66 (1978).
[26] M.B. Einhorn and D.R. Jones, Nucl. Phys. **B196**, 475 (1982); L.E. Ibanez and C. Lopez, *ibid.* **B233**, 511 (1984); H. Arason, D. Castano, B. Keszthelyi, S. Mikaelian, E. Piard, P. Ramond, and B. Wright, Phys. Rev. Lett. **67**, 2933 (1991); A. Giveon, L.J. Hall, and U. Sarid, Phys. Lett. B **271**, 138 (1991); S. Kelley, J.L. Lopez, and D.V. Nanopoulos, *ibid.* **274**, 387 (1992).
[27] P. Langacker and N. Polonsky, Phys. Rev. D **49**, 1454 (1994); W.A. Bardeen, M. Carena, S. Pokorski, and C.E. Wagner, Phys. Lett. B **320**, 110 (1994).
[28] M. Carena, S. Pokorski, and C.E. Wagner, Nucl. Phys. **B406**, 59 (1993).
[29] N. Polonsky, Phys. Rev. D **54**, 4537 (1996).
[30] S. Komine and M. Yamaguchi, Phys. Rev. D **65**, 075013 (2002); U. Chattopadhyay and P. Nath, *ibid.* **65**, 075009 (2002).
[31] W. de Boer, M. Huber, A.V. Gladyshev, and D.I. Kazakov, Eur. Phys. J. C **20**, 689 (2001).
[32] U. Chattopadhyay, A. Corsetti, and P. Nath, Phys. Rev. D **66**, 035003 (2002).
[33] S.M. Barr and I. Dorsner, Phys. Lett. B **556**, 185 (2003).
[34] B. Bajc, G. Senjanovic, and F. Vissani, Phys. Rev. Lett. **90**, 051802 (2003).
[35] A. Masiero, S.K. Vempati, and O. Vives, Nucl. Phys. **B649**, 189 (2003).
[36] M. Drees, hep-ph/9611409; S. Martin, in *Perspectives in Supersymmetry*, edited by G. Kane (World Scientific, Singapore, 1998), hep-ph/9709356; S. Dawson, in *Proceedings of TASI 97*, edited by J. Bagger (World Scientific, Singapore, 1999), hep-ph/9712464.
[37] S. Dimopoulos and D. Sutter, Nucl. Phys. **B452**, 496 (1995); H. Haber, Nucl. Phys. B (Proc. Suppl.) **62**, 469 (1998).
[38] A. Birkedal-Hansen and B.D. Nelson, Phys. Rev. D **67**, 095006 (2003); S.I. Bityukov and N.V. Krasnikov, Phys. At. Nucl. **65**, 1341 (2002); H. Baer, C. Balazs, A. Belyaev, R. Dermisek, A. Mafi, and A. Mustafayev, J. High Energy Phys. **05**, 061 (2002); N. Chamoun, C.S. Huang, C. Liu, and X.H. Wu, Nucl. Phys. **B624**, 81 (2002); C. Balazs and R. Dermisek, hep-ph/0303161.
[39] V. Bertin, E. Nezri, and J. Orloff, J. High Energy Phys. **02**, 046 (2003).
[40] S.K. Soni and H.A. Weldon, Phys. Lett. **126B**, 215 (1983).
[41] A. Datta, M. Guchait, and N. Parua, Phys. Lett. B **395**, 54 (1997); A. Datta, A. Datta, and M.K. Parida, *ibid.* **431**, 347 (1998); E. Accomando, R. Arnowitt, B. Dutta, and Y. Santoso, Nucl. Phys. **B585**, 124 (2000); S. Codoban, M. Jurcisin, and D. Kazakov, Phys. Lett. B **477**, 223 (2000); H. Baer, C. Balazs, S. Hesselbach, J.K. Mizukoshi, and X. Tata, Phys. Rev. D **63**, 095008 (2001).
[42] J. Ellis, T. Falk, K.A. Olive, and Y. Santoso, Nucl. Phys. **B652**, 259 (2003).
[43] H. Baer, M. Diaz, P. Quintana, and X. Tata, J. High Energy Phys. **04**, 016 (2000).
[44] J. Ellis, A. Ferstl, K.A. Olive, and Y. Santoso, Phys. Rev. D **67**, 123502 (2003).
[45] H. Murayama and A. Pierce, Phys. Rev. D **65**, 055009 (2002); B. Bajc, P.F. Perez, and G. Senjanovic, *ibid.* **66**, 075005 (2002); B. Bajc, talk given at Beyond the Desert 02, Oulu, Finland, 2002, hep-ph/0210374.
[46] D. Emmanuel-Costa and S. Wiesenfeldt, hep-ph/0302272.
[47] Super-Kamiokande Collaboration, Y. Hayato *et al.*, Phys. Rev. Lett. **83**, 1529 (1999).
[48] S. Bertolini, F. Borzumati, A. Masiero, and G. Ridolfi, Nucl. Phys. **B353**, 591 (1991).
[49] D.M. Pierce, J.A. Bagger, K.T. Matchev, and R.J. Zhang, Nucl. Phys. **B491**, 3 (1997).
[50] Particle Data Group, D.E. Groom *et al.*, Eur. Phys. J. C **15**, 1 (2000).
[51] G. Belanger, F. Boudjema, A. Pukhov, and A. Semenov, Comput. Phys. Commun. **149**, 103 (2002); http://wwwlapp.in2p3.fr/lapth/micromegas/
[52] P. Gondolo, J. Edsjo, L. Bergstrom, P. Ullio, and T. Baltz, in *York 2000, The Identification of Dark Matter*, edited by N. Spooner and V. Kudryavtsev (World Scientific, Singapore, 2001), p. 318, astro-ph/0012234; http://www.physto.se/edsjo/darksusy
[53] S. Heinemeyer, W. Hollik, and G. Weiglein, hep-ph/0002213.
[54] G. Belanger, F. Boudjema, A. Pukhov, and A. Semenov, hep-ph/0210327.
[55] A.L. Kagan and M. Neubert, Eur. Phys. J. C **7**, 5 (1999); P. Gambino and M. Misiak, Nucl. Phys. **B611**, 338 (2001).
[56] M. Ciuchini, G. Degrassi, P. Gambino, and G. Giudice, Nucl. Phys. **B527**, 21 (1998); G. Degrassi, P. Gambino, and G. Giudice, J. High Energy Phys. **12**, 009 (2000).
[57] S.P. Martin and J.D. Wells, Phys. Rev. D **64**, 035003 (2001).
[58] J. Ellis, T. Falk, and K.A. Olive, Phys. Lett. B **444**, 367 (1998).
[59] A.B. Lahanas, D.V. Nanopoulos, and V.C. Spanos, Phys. Rev. D **62**, 023515 (2000).
[60] P. Binetruy, G. Girardi, and P. Salati, Nucl. Phys. **B237**, 285 (1984).
[61] M. Drees and M.M. Nojiri, Phys. Rev. D **47**, 376 (1993).
[62] J. Rich, M. Spiro, and J. Lloyd-Owen, Phys. Rep. **151**, 239 (1987); T.K. Hemmick *et al.*, Phys. Rev. D **41**, 2074 (1990); T. Yamagata, Y. Takamori, and H. Utsunomiya, *ibid.* **47**, 1231 (1993); P.F. Smith, Contemp. Phys. **29**, 159 (1998).
[63] S.P. Martin and J.D. Wells, Phys. Rev. D **67**, 015002 (2003).
[64] CDMS Collaboration, R. Abusaidi *et al.*, Phys. Rev. Lett. **84**, 5699 (2000); A. Benoit *et al.*, Phys. Lett. B **545**, 43 (2002); EDELWEISS Collaboration, G. Sanglard, talk given at the XXXVIIIth Rencontres de Moriond on ElectroWeak Interactions and Unified Theories, 2003; ZEPLIN Collaboration, R. Luscher, *ibid*.
[65] MACRO Collaboration, T. Montaruli, hep-ex/9905021; O.V. Suvorova, hep-ph/9911415; Super-Kamiokande Collaboration, A. Habig, hep-ex/0106024; J. Edsjo, astro-ph/0211354.

[66] See, e.g., M. Kamionkowski, K. Griest, G. Jungman, and B. Sadoulet, Phys. Rev. Lett. **74**, 5174 (1995); L. Bergstrom, J. Edsjo, and P. Gondolo, Phys. Rev. D **58**, 103519 (1998); V. Bertin, E. Nezri, and J. Orloff, Eur. Phys. J. C **26**, 111 (2002).
[67] V. Barger and C.E.M. Wagner *et al.*, hep-ph/0003154.
[68] K. Hagiwara *et al.*, Phys. Rev. D **66**, 010001 (2002); C.T. Sachrajda, Nucl. Instrum. Methods Phys. Res. A **462**, 23 (2001).
[69] H. Baer, J. Ferrandis, K. Melnikov, and X. Tata, Phys. Rev. D **66**, 074007 (2002).
[70] M.E. Gomez, G. Lazarides, and C. Pallis, Nucl. Phys. **B638**, 165 (2002).
[71] M. Carena, D. Garcia, U. Nierste, and C.E.M. Wagner, Nucl. Phys. **B577**, 88 (2000).
[72] T. Blazek, R. Dermisek, and S. Raby, Phys. Rev. Lett. **88**, 111804 (2002); Phys. Rev. D **65**, 115004 (2002).
[73] ALEPH Collaboration, R. Barate *et al.*, Phys. Lett. B **429**, 169 (1998); BELLE Collaboration, K. Abe *et al.*, *ibid.* **511**, 151 (2001); CLEO Collaboration, S. Chen *et al.*, Phys. Rev. Lett. **87**, 251807 (2001).
[74] F.M. Borzumati, M. Olechowski, and S. Pokorski, Phys. Lett. B **349**, 311 (1995).
[75] R. Barbieri and G.F. Giudice, Phys. Lett. B **309**, 86 (1993).
[76] ALEPH, DELPHI, L3 and OPAL Collaborations, ''The LEP Higgs Working Group for Higgs Boson Searches,'' hep-ex/0107029, LHWG Note/2001-03; http://lephiggs.web.cern.ch/LEPHIGGS/www/Welcome.html
[77] K. Hagiwara, A.D. Martin, D. Nomura, and T. Teubner, Phys. Lett. B **557**, 69 (2003); M. Davier, S. Eidelman, A. Hocker, and Z. Zhang, Eur. Phys. J. C **27**, 497 (2003).
[78] A. Nyffeler, talk given at the XXXVIIIth Rencontres de Moriond on ElectroWeak Interactions and Unified Theories, 2003.
[79] S. Narison, hep-ph/0303004.
[80] J. Ellis and K.A. Olive, Phys. Lett. B **514**, 114 (2001).
[81] T. Nihei, L. Roszkowski, and R.R. de Austri, J. High Energy Phys. **03**, 031 (2002).
[82] T. Nihei, L. Roszkowski, and R.R. de Austri, J. High Energy Phys. **07**, 024 (2002).